Contrib Mineral Petrol (1990) 105:255–274

Contributions to Mineralogy and Petrology

Mantle derivation of Archean amphibole-bearing granitoid and associated mafic rocks: evidence from the southern Superior Province, Canada

Richard H. Sutcliffe[1], **Alan R. Smith**[1], **William Doherty**[1], **and Robert L. Barnett**[2]

[1] Ontario Geological Survey, 77 Grenville Street, Toronto, Canada, M7A-1W4
[2] Department of Geology, University of Western Ontario, London, Canada, N6A-5B7

Received July 14, 1989 / Accepted February 26, 1990

Abstract. Amphibole-bearing, Late Archean (2.73–2.68 Ga) granitoids of the southern Superior Province are examined to constrain processes of crustal development. The investigated plutons, which range from tonalite and diorite to monzodiorite, monzonite, and syenite, share textural, mineralogical and geochemical attributes suggesting a common origin as juvenile magmas. Despite variation in modal mineralogy, the plutons are geochemically characterized by normative quartz, high Al_2O_3 ($>$ 15 wt%), Na-rich fractionation trends (mol $Na_2O/K_2O > 2$), low to moderate Rb (generally <100 ppm), moderate to high Sr (200–1500 ppm), enriched light rare earth elements (LREE) (Ce_N generally 10–150), fractionated REE (Ce_N/Yb_N 8–30), Eu anomaly (Eu/Eu*) ~1, and decreasing REE with increasing SiO_2. The plutons all contain amphibole-rich, mafic-ultramafic rocks which occur as enclaves and igneous layers and as intrusive units which exhibit textures indicative of contemporaneous mafic and felsic magmatism. Mafic mineral assemblages include: hornblende + biotite in tonalites; augite + biotite ± orthopyroxene ± pargasitic hornblende or hornblende + biotite in dioritic to monzodioritic rocks; and aegirine-augite ± silicic edenite ± biotite in syenite to alkali granite. Discrete plagioclase and microcline grains are present in most of the suites, however, some of the syenitic rocks are hypersolvus granitoids and contain only perthite. Mafic–ultramafic rocks have REE and Y contents indicative of their formation as amphibole-rich cumulates from the associated granitoids. Some cumulate rocks have skeletal amphibole with $X_{Mg}(Mg/(Mg+Fe^{2+}))$ indicative of crystallization from more primitive liquids than the host granitoids. Geochemical variation in the granitoid suites is compatible with fractionation of amphibole together with subordinate plagioclase and, in some cases, mixing of fractionated and primitive magmas. Mafic to ultramafic units with magnesium-rich cumulus phases and primitive granitoids (mol $MgO/(MgO+0.9\,FeO^{TOTAL})$) from 0.60 to 0.70 and Cr >150 ppm) are comagmatic with the evolved granitoids and indicate that the suites are mantle-derived. Isotopic studies of Archean monzodioritic rocks have shown LREE enrichment and initial $^{143}Nd/^{144}Nd$ ratios indicating derivation from mantle sources enriched in large ion lithophile elements (LILE) shortly before melting. Mineral assemblages record lower P_{H_2O} with increased alkali contents of the suites. This evidence, in conjunction with experimental studies, suggests that increased alkali contents may reflect decreased P_{H_2O} during mantle melting. These features indicate that ~2.73 Ga tonalitic rocks are derived from more hydrous mantle sources than ~2.68 Ga syenitic rocks, and that the spectrum of late Archean juvenile granitoid rocks is broader than previously recognized. Comparison with Phanerozoic and recent plutonic suites suggests that these Archean suites are subduction related.

Introduction

The origin of Late Archean plutonism is fundamental to understanding the evolution of the early continental crust. Geochemical investigations of Archean tonalitic and monzodioritic to syenitic rocks have emphasized the characteristic highly-fractionated rare earth element (REE) patterns and depletion in heavy REE (HREE) (Arth and Hanson 1972, 1975; Martin 1986). Most models propose that these rocks are derived from melting of mafic rocks, usually with garnet as a residual phase (e.g., Arth and Hanson 1975; Barker and Arth 1976; Martin 1986). Alternatively, some tonalitic and monzodioritic rocks may be produced by partial melting of the mantle. Arth et al. (1978) suggested that a Proterozoic tonalite suite in Finland was derived by fractionation of basaltic magma. Shirey and Hanson (1984) and Stern et al. (1989) proposed that some Late Archean monzodioritic rocks are derived by direct melting of LILE-enriched mantle.

This contribution examines the field relationships, petrography, and geochemistry of examples of 2.7 Ga

---

Offprint requests to: R.H. Sutcliffe

amphibole-bearing tonalitic, monzodioritic and syenitic plutonic rocks in the Wabigoon and Abitibi Subprovinces of the southern Superior Province. The geological compilation map of Ontario (Ontario Geological Survey 1990) indicates that these types of rocks comprise up to 25% of greenstone-granitoid terranes of the Superior Province of Ontario and therefore should be considered as a significant component of models that describe custal evolution. The plutons were studied during several Ontario Geological Survey mapping projects designed to investigate the nature and origin of Late Archean magmatism. During the mapping it was realized that, whereas the plutonic suites have a diverse range of modal mineralogy, they share many common field, mineralogical, and compositional attributes. Based on these characteristics we suggest that a broad compositional range of late Archean granitoids are juvenile and formed by similar processes. In detail, however, it is apparent that these plutons are the products of a range of parental-magma compositions and source compositions.

In this paper mantle-derived magmas, which may subsequently be fractionated, are referred to as juvenile. Comagmatic is used to describe rocks directly related by fractionation processes, whereas cogenetic is used in a more general sense to relate rocks formed during a common tectono-thermal event. The plutonic rocks are classified according to the IUGS system (Streckeisen 1976) and granitoid is used as a general term for mesocratic to leucocratic plutonic rocks. All ages are U/Pb zircon dates unless otherwise noted.

Geology

The tonalitic rocks in the Lac des Iles (LDI) area and the monzodioritic Jackfish Lake Pluton (JLP) are from the Wabigoon Subprovince. A tonalitic suite from the Abitibi Batholith (AB) and a syenitic suite from the Otto Stock (OS) are from the Abitibi Subprovince (Fig. 1).

The AB (Fig. 2a) is an elliptical pluton (1200 km^2) intrusive into metavolcanic rocks of the Abitibi Greenstone Belt. The composite intrusion consists of: early hornblende diorite to quartz diorite, gabbro and hornblendite; foliated to massive biotite-hornblende tonalite to granodiorite; and late microcline-porphyritic granodiorite (Smith and Sutcliffe 1988). A porphyritic granodiorite from the AB has been dated at 2689 $+2.7/-2.3$ Ma (Mortensen 1987). The biotite – hornblende tonalite to granodiorite, which is predominant in the western part of the AB, is examined in this study.

The OS (Fig. 2b) is one of several alkalic intrusions exposed near the Kirkland Lake-Larder Lake Deformation Zone. The OS is an approximately circular stock (95 km^2) intrusive into metavolcanic rocks. Syenite and alkali granite units are predominant in the intrusion and are associated with hornblendite, pyroxene – hornblendite and mela-syenite units (Smith and Sutcliffe 1988). Nepheline syenite comprises $<5\%$ and forms a narrow marginal phase (Lovell 1972). An age of 2680 ± 1 Ma was obtained from the OS using zircon and titanite (Corfu et al. 1989).

The hornblende tonalite at LDI (Sutcliffe 1989, Fig. 1) is an elliptical pluton (150 km^2) intrusive into older gneissic biotite tonalite. A U/Pb zircon age of 2729 ± 2 Ma has been obtained for the tonalite (unpublished data, D.W. Davis, Royal Ontario Museum, personal communication).

The JLP (Fig. 2c) is a crescentic pluton (500 km^2) intrusive into tonalitic gneiss and mafic metavolcanic rocks (Blackburn 1976; Edwards 1983a, 1983b). The pluton ranges from diorite to monzodiorite, quartz monzodiorite, monzonite and granodiorite (Sutcliffe and Fawcett 1980; Longstaffe et al. 1980, 1982). Shirey and Hanson (1984) included a dioritic phase of the JLP in examples of magmatism related to melting of LILE-enriched mantle. An age of 2698 ± 1 Ma has been obtained from monzodioritic rocks of the pluton (unpublished data, D.W. Davis, personal communication).

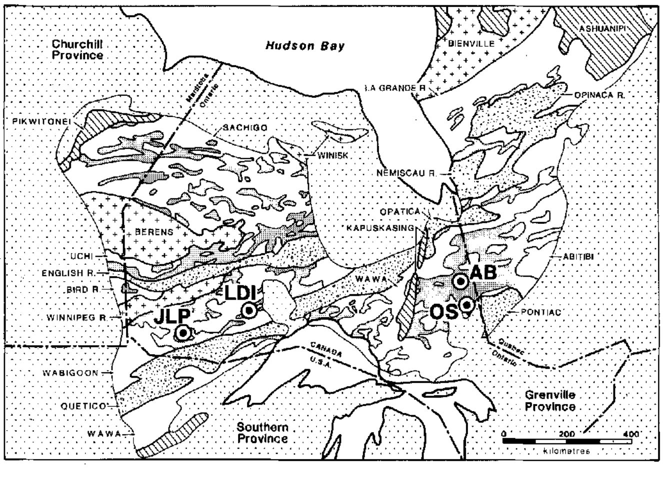

Fig. 1. Location map for the study areas showing subprovinces of the Superior Province. Plutons investigated in this study are: Jackfish Lake Pluton (*JLP*); Lac des Iles (*LDI*); Otto Stock (*OS*); and Abitibi Batholith (*AB*)

All of the granitoids are spatially associated with mafic to ultramafic plutons, dikes, layers and enclaves (Fig. 3). At LDI mafic dikes show gradational relationships and net-vein textures indicative of contemporaneous mafic and felsic magmatism (Sutcliffe 1989). Gravity studies at LDI indicate that the mafic-ultramafic intrusions, such as the LDI Complex, are shallow (3–4.5 km thick) lopoliths which locally underplate the tonalite (Gupta and Sutcliffe 1990).

Mafic units, lithologically similar to mafic-ultramafic intrusions in the LDI area, are also present within the AB, where a gabbronorite to hornblende gabbro and hornblendite intrusion (45 km^2) is present within the hornblende tonalite. In addition, hornblende diorite with abundant enclaves of hornblendite occurs on the western side of the AB.

Mafic to ultramafic amphibole- and pyroxene-rich units comprise approximately 9% of the OS and form an oval body approximately 2 km in diameter in the core of the intrusion and also form smaller lenses and pods within the intrusion. Syenitic and dioritic enclaves within the mafic core are evidence of the late intrusive nature of the mafic core. In the southern part of the stock, however, a layered sequence of pyroxene – hornblendite, mela-diorite, and syenite indicates that some amphibole-rich rocks are in situ cumulates (Fig. 3).

In the JLP, mafic units consist of mela-quartz monzonite which is a volumetrically minor intrusive phase into monzodioritic rocks of the pluton and into gneissic tonalite country rocks south of the pluton. Ultramafic hornblendite and pyroxene – hornblendite enclaves, ranging from a few centimentres to 1 kilometre, are abundant throughout the JLP and comprise approximately 10–15% of the intrusion.

Kersantite (biotite – plagioclase lamprophyre) dikes are spatially associated with the JLP (Edwards 1983a) and the OS (Lovell 1972). Spessartite (amphibole – plagioclase lamprophyre) and kersantite dikes are also abundant at the LDI (Sutcliffe 1989). These dikes are generally less than 1 m wide, dip steeply, commonly have 1 to 2 cm wide foliated margins, and locally, such as at the LDI, show textural evidence of being emplaced prior to consolidation of the tonalite host (Fig. 3). A titanite from a lamprophyre dike

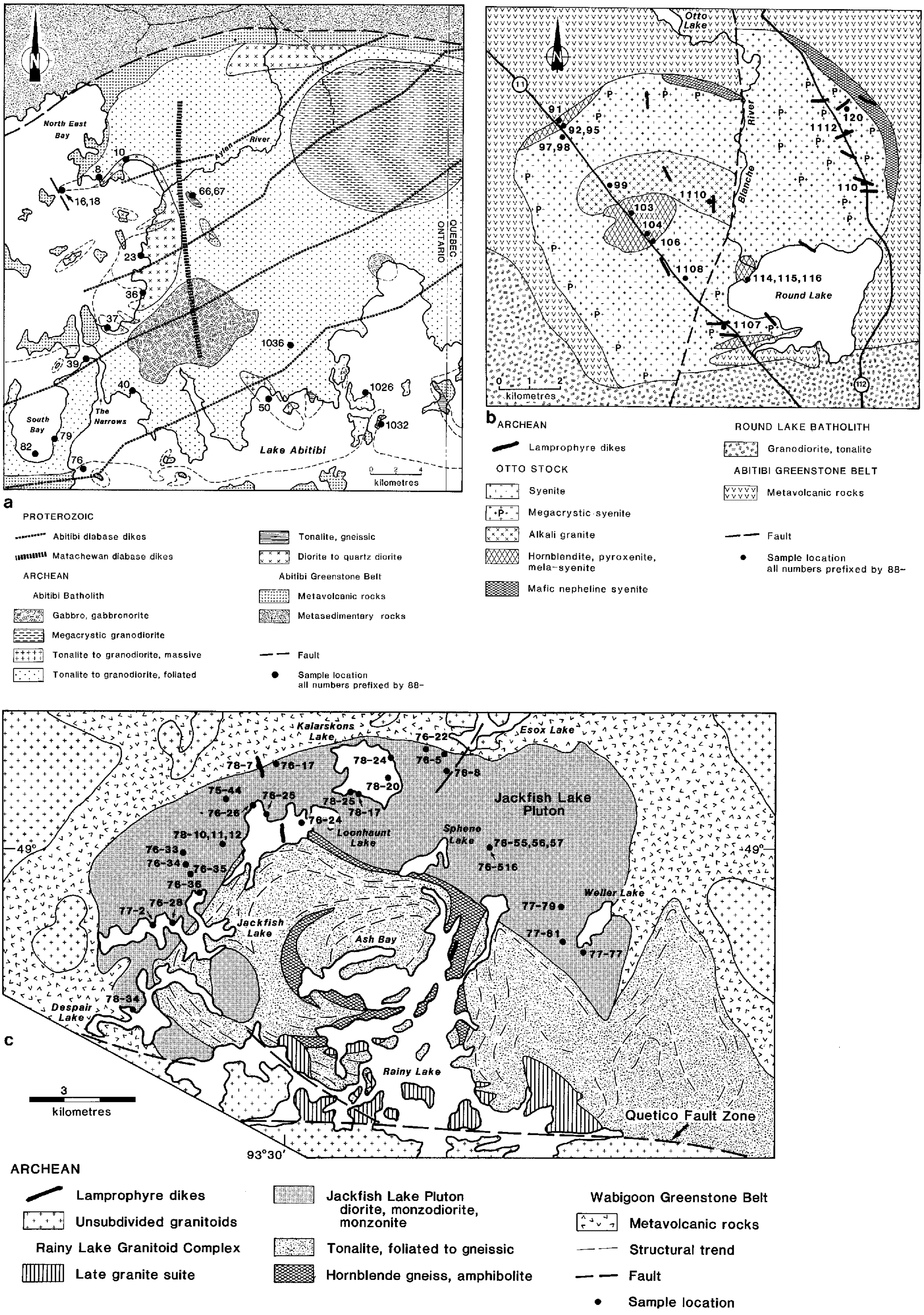

Fig. 2a–c. Geological maps of the study areas. Geology of: **a AB** from Smith and Sutcliffe (1988); **b OS** from Smith and Sutcliffe (1988) and Lovell (1972); **c JLP** from Sutcliffe and Fawcett (1980). See Sutcliffe (1989) for **LDI**

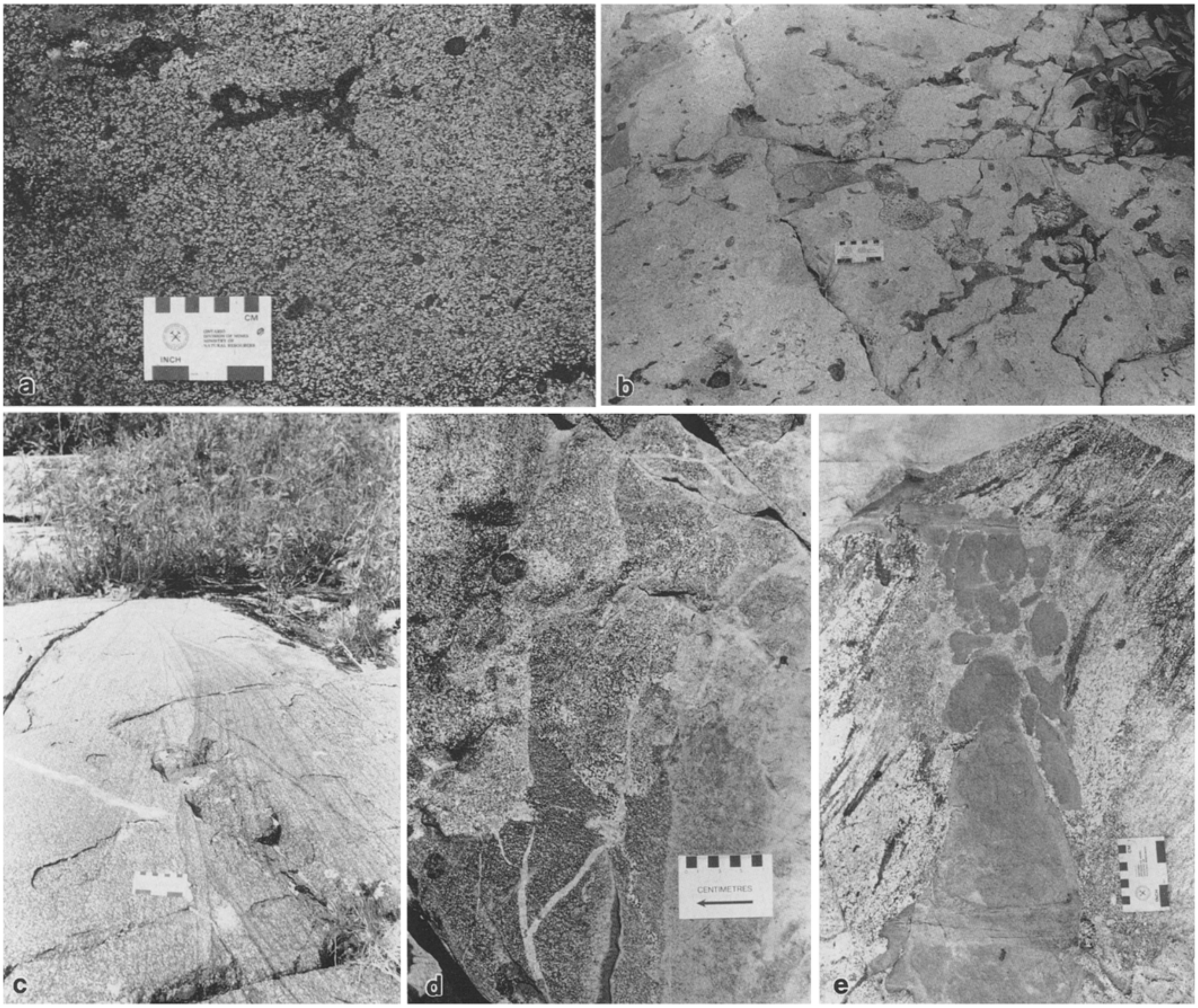

Fig. 3a–e. Photographs of relationships between mafic and felsic rocks. **a** Hornblendite clots and small irregular enclaves in monzodiorite, *JLP*. **b** Rounded and irregular hornblendite to diorite clots and enclaves in syenite, *OS*. **c** Cross-bedded and trough-bedded hornblende-rich layers in syenite, *OS*. **d** Irregular and gradational contact relations between tonalite and quartz diorite, west side of *AB*. **e** Disaggregated mafic dike in hornblende tonalite, *LDI*. Note loss of foliation in remobilized felsic material adjacent to dike

south of Kirkland Lake which is intrusive into syenite has an age of 2674±2 Ma, similar to late tectonic intrusions in the area (Wyman and Kerrich 1989).

Petrography

Modal analyses of representative rocks analyzed for this study are given in Table 1 and Fig. 4. Table 2 summarizes details of mineral assemblages and textures.

The granitoid rocks are generally characterized by medium- to coarse-grained, hypidiomorphic, massive to weakly foliated textures. Tabular plagioclase is subhedral, and displays moderate to strong oscillatory zoning locally (AB, LDI, JLP). The most common mafic mineral assemblage is biotite+hornblende (LDI, AB, JLP) with hornblende locally rimming augite (JLP). The less common assemblages are biotite+augite+/−orthopyroxene (JLP) (Fig. 5c) and aegirine−augite+biotite+/−amphibole (OS). Coarse hornblende grains up to 2 cm in length are common in both the LDI and the AB tonalites (Fig. 5a). Microcline and quartz are usually present as anhedral, interstitial grains. As the proportion of microcline increases, however, microcline occurs as poikilitic megacrysts up to 2 cm in length enclosing plagioclase, quartz and mafic minerals (JLP, OS). Most of the OS is characterized by tabular 2–4 mm strongly perthitic microcline with albite exsolution (Fig. 5d). Some OS syenites, however, contain discrete grains of plagioclase and microcline. In all of the plutons accessory apatite, titanite, and zircon most commonly occur as inclusions in mafic minerals. Magnetite is the predominant oxide phase.

Mafic to ultramafic units and enclaves consist of medium- to coarse-grained amphibolite to pyroxenite with massive allotriomorphic textures (Fig. 5b, f) and interstitial biotite, plagioclase, carbonate and quartz with minor apatite, titanite and opaques. Mela-granitoid units are gradational between the tonalites, monzodiorites, syenites, and the mafic-ultramafic rocks. They are charac-

Table 1. Modal analysis and estimates of rocks from the Abitibi Batholith, Jackfish Lake Pluton and Otto Stock

	88-37	88-66	88-39	88-40	88-08	88-50	78-56	76-36	78-25	78-20	77-79	75-44	78-17	78-55	88-1108	88-99	88-120	88-103	88-104	88-114	88-1112	78-7[c]
Plagioclase[a]	48.0	49.8	59.7	57.2	59.6	65.0	61.8	57.9	53.4	55.2	53.2	15.1	1.0	< 1.0	40.3	–	4.2	30.0	3.3	1.5	27.9	–
Microcline	–	–	–	–	tr	10.0	0.4	4.8	11.7	17.7	21.3	11.3	–	–	44.3	77.7[b]	60.4[b]	–	–	–	–	–
Quartz	13.2	30.4	27.9	25.5	35.0	25.0	0.4	0.1	6.1	1.1	17.3	7.9	–	–	–	18.4	2.0	tr	–	0.1	–	–
Amphibole	24.5	12.1	5.6	5.4	2.5	tr	0.1	30.8	16.9	19.8	0.2	22.8	85.0	68.0	tr	0.7	–	35.0	32.8	77.5	20.0	60.0
Biotite	13.2	5.1	5.9	10.5	1.3	5.0	8.6	4.2	4.9	tr	5.3	–	tr	< 1.0	0.3	–	10.4	10.0	30.8	–	46.6	25.0
Pyroxene	–	–	–	–	–	–	27.6	0.1	4.2	4.1	–	42.1	10.0	28.0	14.0	2.5	18.8	20.0	32.3	7.4	–	–
Chlorite	–	1.1	–	–	–	–	–	0.1	–	0.2	0.2	–	–	< 1.0	–	–	–	–	–	3.8	–	–
Epidote	–	0.2	–	tr	0.4	–	–	1.0	1.6	0.4	1.6	0.3	tr	–	–	–	–	–	0.4	2.2	0.8	–
Carbonate	–	–	–	–	–	–	–	–	–	–	–	–	–	–	–	–	–	–	–	1.0	3.9	–
Sphene	–	0.9	tr	0.5	0.7	tr	–	0.4	0.4	0.5	0.5	0.2	1.0	–	0.7	0.6	2.3	tr	tr	0.1	0.4	–
Zircon	–	–	–	tr	–	–	–	0.1	tr	–	tr	–	–	–	tr	–	–	–	–	–	–	–
Apatite	–	0.2	tr	0.5	–	tr	0.2	0.5	0.2	0.4	0.1	0.2	2.0	< 1.0	tr	tr	1.4	tr	tr	–	–	tr
Opaques	1.0	tr	0.9	0.3	–	tr	0.9	tr	0.6	0.6	0.4	–	–	2.0	–	–	0.5	3.0	0.2	5.8	0.3	tr
Total Pts	1049	1107	1022	1137	892	est	2040	2049	2025	2071	2039	2050	est.	est	1313	1078	997	est	1109	1324	1210	est

[a] Includes sericite alteration; [b] Perthite; [c] Includes 15% serpentine after olivine.

88-37	Biotite – hornblende quartz diorite **AB**
88-39	Biotite – hornblende tonalite, **AB**
88-40	Hornblende – biotite tonalite, **AB**
88-08	Biotite – hornblende tonalite, quartz-feldspar phyric, **AB**
88-66	Biotite – hornblende tonalite, **AB**
88-50	Biotite granodiorite, **AB**
78-56	Biotite – augite diorite, **JLP**
76- 36	Biotite – hornblende diorite, **JLP**
78- 25	Biotite – hornblende monzodiorite, **JLP**
78- 20	Biotite – hornblende monzodiorite, **JLP**
77- 79	Biotite – hornblende monzonite, **JLP**
75- 44	Mela-monzonite, cumulate, **JLP**
78- 17	Clinopyroxene – hornblendite enclave, cumulate, **JLP**
78- 55	Opx – cpx – hornblendite enclave; cumulate, **JLP**
88-103	Mela – diorite, cumulate, **OS**
88- 104	Clinopyroxene – hornblendite, central core, cumulate, **OS**
88-1108	Aegirine – augite syenite, **OS**
88- 99	Aegirine – augite alkali granite, **OS**
88- 120	Aegirine – augite mela – syenite, cumulate, **OS**
88- 114	Hornblendite, cumulate layer in syenite, **OS**
88-1112	Lamprophyre dike, intrudes **OS**
78- 7	Lamprophyre dike, intrudes **JLP**

terized by euhedral, prismatic pyroxenes and amphibole with interstitial feldspar and quartz. Clinopyroxene and amphibole in these rocks commonly exhibit a distinctive skeletal texture (Fig. 5e). At LDI these skeletal textures are attributed to supercooling during mixing of magmas (Sutcliffe 1989).

Geochemistry

Analytical methods

Whole rock major and trace element analyses were done at the Geoscience Laboratories, Ontario Geological Survey, Toronto (AB, OS, LDI) and at the University of Toronto (JLP). Granitoid samples weighing 1 to 2 kg were stripped of weathered surfaces before crushing. Major elements were determined by XRF using fusion beads. Trace elements Zr, Rb, Sr were determined by XRF on pressed pellets. Cr and Ni were determined by the atomic absorbtion flame method. Precision and detection limits for major and trace elements are as reported by Sutcliffe et al. (1989). Rare earth elements (REE) and Y were determined at the Ontario Geological Survey using ICP-mass spectrometry. Details of the analytical precision, which is approximately 4% at chondritic abundances, and accuracy of this procedure are reported by Doherty (1989).

Mineral phases from the AB, OS and LDI were analyzed at the University of Western Ontario using a MAC 400 electron microprobe fitted with a Krisel control automation system using Magic IV correction procedures. Operating conditions, detection limits and precision are as reported by Sutcliffe et al. (1989). Amphibole separates, estimated to be at least 99% pure, were obtained by magnetic separation and hand picking of individual grains of the 100–140 mesh size fraction. Approximately 0.01–0.04 g of separate was analyzed for trace elements by ICP-mass spectrometry.

Rock Chemistry

Representative whole rock analyses from the AB, JLP and OS are given in Table 3. Analyses of the LDI tonalitic rocks are given in Sutcliffe (1989). Group averages and ranges for the suites are given in Table 4 to facilitate comparison. It should be noted that many of the rocks, particularly the melagranitoids and mafic enclaves, do not represent liquid compositions. These and other rocks which are the product of crystal accumulation are identified in Table 3. Although deviations from liquid compositions in the granitoid rocks may also be present as a result of crystal accumulation and late migration of fluids, Fig. 6 shows that all of the granitoids have trends within the calc-alkaline field, with the LDI and AB being FeO-rich relative to the JLP and OS. The CaO – Na_2O – K_2O diagram (Fig. 6) illustrates that the LDI and AB suites have Na-rich trondhjemitic trends whereas the JLP and OS are more K-rich. The OS is alkali-calcic whereas the other plutons are calc-alkalic (classification of Peacock 1931).

Both AB and LDI tonalitic suites are characterized by Al_2O_3 generally greater than 15 wt%, comparable to the high-Al_2O_3 type tonalite of Barker and Arth (1976). The tonalites have mol $Al_2O_3/(Na_2O+K_2O+CaO)$ close to unity with mol Na_2O/K_2O generally >4.0.

Rocks of monzodioritic and syenitic composition are also characterized by high Al_2O_3 but all are metaluminous. With increasing SiO_2, $Al_2O_3/(Na_2O+K_2O+CaO)$ increases. Molecular Na_2O/K_2O is lower than in

Table 2. Summary of petrography of lithologies from Abitibi Batholith, Jackfish Lake Pluton and Otto Stock

Rock Type	Texture	Grain Size	Feldspars	Mafic Minerals	Accessory Phases	Alteration
Abitibi Batholith						
Tonalite, granodiorite	Hypidiomorphic, massive to weakly foliated	Medium to coarse	pl (subhedral, tabular, oscillatory zoning common) ± mc (anhedral, interstitial)	hb (subhedral to prismatic, green pleochroic 2 mm to 2 cm) + bio (green-brown pleochroic)	tit, ap, mgt, zir	pl to ep, ser minor chl
Quartz diorite						
Jackfish Lake Pluton						
Bio-aug diorite	Hypidiomorphic, equigranular, massive to foliated, mafic minerals in aggregates	Medium to coarse	pl (subhedral, tabular, local oscillatory zoning) ± mc (interstitial)	aug (prismatic) + bio (red-brown pleochroic) ± opx	tit, ap, mgt, zir	pl to ep, ser hp+bio to ep+chl, cpx to uralite
Bio-hb diorite				hb (blue green pleochroic, locally mantles aug) + bio (green brown pleochroic)		
Monozdiorite			pl (subhedral, tabular, sodic rims) + mc (interstitial to megacrystic, replaces pl)			
Monzonite	Locally mc megacrystic	Medium to coarse (mc to 2 cm		as above, no cpx		as above, more intense
Mela-monzonite	Allotriomorphic	Coarse	pl + mc (both interstitial)	hb + aug (euhedral, skeletal) ± bio	ox, tit	
Hornblendite	Hypidiomorphic to allotriomorphic massive	Medium	pl (interstitial)	hb (green pleochroic) ±aug hb (brown pleochroic) + aug ± opx	tit, ox, ap, carb (interstitial)	ep, chl, uralite
Otto Stock						
Syenite	Hypidiomorphic, massive to weak foliation	Medium to coarse	per (hypersolvus texture)	aegirine-aug (subhedral, prismatic) + bio (green-brown pleochroic) ± amph (blue-green brown pleochroic)	tit, mgt, ap, zir	ep, ser, chl
Alkali granite			or pl (subhedral) + mc (subhedral) (subsolvus texture)			
Porph syenite		mc to 2 cm	mc megacrysts			
Mela-diorite to syenite	Allotriomorphic, massive	Medium to coarse	pl (interstitial) ± mc (interstitial)	as above, aug and amph locally skeletal	tit, mgt, ox, zir carb (interstitial)	
Hornblendite				amph (green pleochroic) ± aug (overgrown by amph) aegirine – aug + bio (interstitial)		

Abbreviations: pl – plagioclase; mc – microclinie; hb – hornblende; bio – biotite; aug – augite, opx – orthopyroxene; tit – titanite; ap – apatite; mgt – magnetite; ox – oxides; zir – ziron; ep – epidote; ser – sericite; chl – chlorite; carb – carbonate; amph – amphibole; per – perthite. Where present quartz is anhedral and interstitial.

the tonalitic rocks but is >1 in all cases. Syenitic rocks from OS contain from 0.2–14% normative quartz. Most rocks from JLP are also quartz normative, however, some dioritic rocks from the pluton contain normative olivine.

The tonalitic rocks have moderate Sr (213–706 ppm) and low Rb (12–49 ppm). Monzodioritic and syenitic rocks have moderate to high Sr (253–1539 ppm) and low to moderate Rb (28–195 ppm). Zr and Y contents and Rb/Sr and K/Rb ratios are broadly comparable in all suites.

Harker variation diagrams (Fig. 7) illustrate similar patterns for many of the suites. All suites exhibit negative correlation of major oxides and trace elements (TiO_2, $FeO^{total(t)}$, MnO, MgO, CaO, P_2O_5, Cr, Ni and Y) with SiO_2. Mafic to ultramafic enclaves and melanocratic rocks generally have SiO_2 less than 55–60 wt%. These rocks show steep negative correlation of MgO, Ni and Cr vs SiO_2. Rb, Zr, and K_2O in the granitoids generally correlate positively with SiO_2, however, LDI tonalites are an exception to this (Sutcliffe 1989). Al_2O_3 is approximately constant or has negative correlation

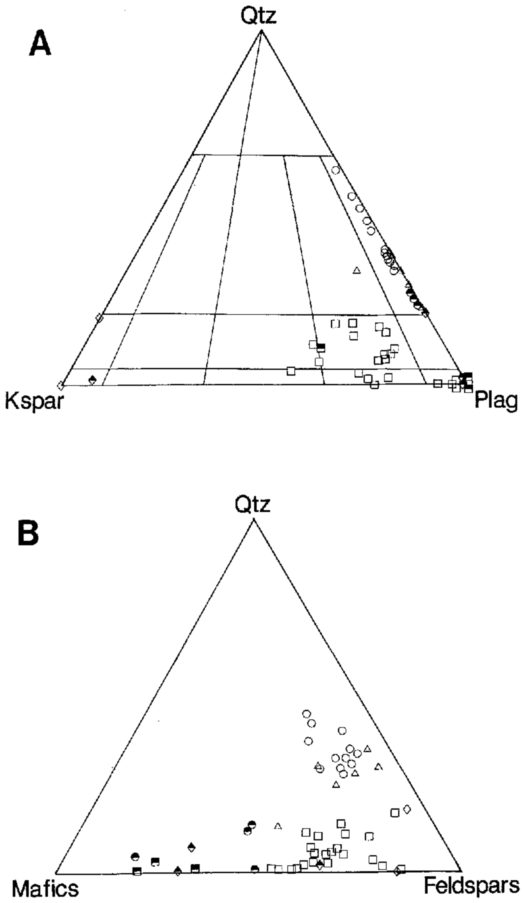

Fig. 4a, b. Modal analyses of plutonic rocks plotted on diagrams showing **a** quartz – plagioclase – alkali feldspar and **b** quartz – feldspar – mafics. Fields correspond to classification system of Streckeisen (1976). *Triangles* – **AB**; *circles* – **LDI**; *squares* – **JLP**; *diamonds* – **OS**. *Open symbols* – granitoids; *half-filled symbols* – mela-granitoids; *filled symbols* – mafic to ultramafic units

with SiO_2 in the granitoid rocks, but shows a weak positive correlation in the mafic rocks. Sr is also constant or shows slight depletion with increasing SiO_2 in the granitoids of most suites. ($Na_2O + K_2O$) shows regular positive correlation with SiO_2 and is lower in melanocratic phases relative to the granitoids.

The granitoids of all suites display similar REE patterns (Fig. 8) characterized by moderate fractionation of Ce_N/Yb_N (8–30) (N = chondrite normalized) and generally no significant Eu anomaly. Within suites, total REE decrease with increasing SiO_2. The LDI and Ab tonalitic suites have comparable REE abundances and lower total REE than the JLP and OS. Analyses of syenite and alkali granite from OS have similar REE abundances to monzonitic rocks of JLP.

Mela-granitoid phases and mafic enclaves from LDI, JLP and OS generally have similar patterns characterized by high total REE and, in particular, high HREE in comparison to the associated granitoids. A distinctive feature of most of the melanocratic phases and mafic enclaves is $La_N < Pr_N$. Melanocratic rocks of OS, however, have considerable variation in LREE abundances. The lowest LREE concentrations are in sample 88–114, a hornblendite layer in syenite, which has $La_N < Pr_N$ comparable to LDI and JLP melanocratic phases. Enriched patterns of LREE are obtained from the central pyroxene – hornblendite core of the intrusion. Extreme LREE-enrichment characterizes sample 88–120, an aegirine – augite rich phase with microcline megacrysts.

Lamprophyre dikes from OS, JLP and the more mafic dikes at LDI have contents of 40–50 wt% SiO_2, 0.5–0.7 wt% TiO_2, 0.4–0.5 wt% P_2O_5, Mg′ (Mg′ = mol $MgO/(MgO + 0.9\ FeO^t)$) of 0.68–0.71, and have elevated Cr, Ni, Sr and LREE comparable to other Archean calc-alkaline lamprophyres (Wyman and Kerrich 1989). The samples analyzed in this study have mol $Na_2O/K_2O > 1$ and therefore are not clearly shoshonitic. High CO_2 and H_2O contents reflect the high modal abundances of mica and carbonate and may be primary.

Mineral chemistry

Representative amphibole and pyroxene analyses for tonalitic, monzodioritic, and syenitic rocks are given in Table 5. Using the classification of Leake (1978) all amphiboles are calcic. Amphiboles in tonalitic and monzodioritic rocks vary from actinolite to magnesio-hornblende and ferro-hornblende with $(Na + K)_A$ (A = A site of standard amphibole formula) less than 0.50. Actinolite and actinolitic-hornblende have higher X_{Mg} ($Mg/(Mg + Fe^{2+})$) than associated hornblende. This variation apparently reflects the reaction of clinopyroxene and liquid to form hornblende with actinolite being an intermediate stage. Amphiboles in dioritic and hornblende-rich rocks from both the LDI area and AB are generally edenitic- to pargasitic-hornblende and marginally hastingsitic-hornblende with $(Na + K)_A$ greater than 0.50. Amphiboles from OS have considerable variation in alkali elements and are more Fe^{3+}-rich than the other suites. Amphiboles from OS mafic to ultramafic enclaves vary from hastingsitic-hornblende [$Fe^{3+} > Al^{iv}$ and $(Na + K)_A > 0.50$] with less aluminous hornblende and edenite rims (eg. samples 88–104, 88–114). One analyzed grain from sample 88–104 has a kaersutite core. Amphibole coexisting with aegirine – augite in alkali granite has the highest alkali content of the analyzed amphiboles and is sodium-rich silicic edenite with Na_B ranging from 0.62–0.64.

Hornblende separates from granitoid rocks (Table 6 and Fig. 8) have low Rb (1–4 ppm), high Y (24–68 ppm), high total REE and HREE, $La_N < Pr_N$ and moderate Ce_N/Yb_N comparable to the melanocratic granitoid and mafic enclave phases. Eu/Eu* (0.51–0.35) is somewhat lower than the melanocratic and mafic phases, however, all are characterized by Eu/Eu* < 1.

Based on analysis of five rocks, pyroxenes from the OS range in composition from augite to aegirine-augite with up to 40% aegirine component. The most aegirine-rich pyroxenes are from the granitoids, while the most Mg-rich and aegirine-poor are from the central hornblende – pyroxenite core.

Clinopyroxene from JLP is augite, with the most Mg-

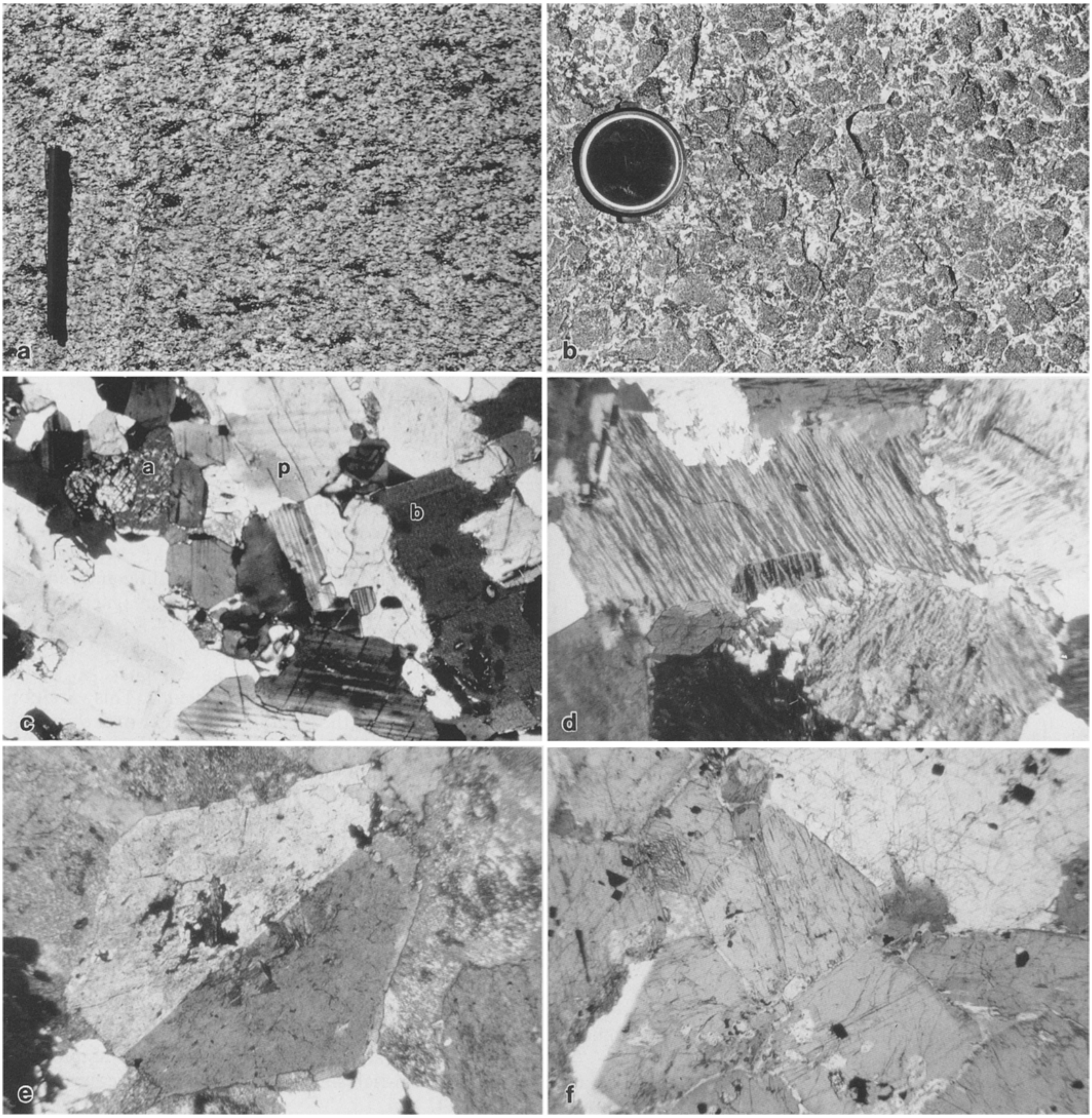

Fig. 5a–f. Photomicrographs and photographs of textures in the plutonic rocks. **a** Blocky hornblende in foliated, biotite–hornblende tonalite, **AB**. **b** Coarse poikilitic hornblende with interstitial felsic phases, pyroxene hornblendite. **OS**. **c** Hypidiomorphic biotite–augite diorite, **JLP**. Biotite (*b*), augite (*a*), and plagioclase (*p*) are labelled. **d** Perthite in alkali granite, **OS**, sample 88–99. **e** Euhedral skeletal hornblende surrounded by variably sericitized plagioclase, **LDI**, sample 85–235. **f** Allotriomorphic pyroxene–hornblendite enclave, **OS**, hornblende includes augite, sample 88–114. Figures **5c–f** is with crossed polars and have a field of view of 4.2 mm

rich pyroxenes occurring as diopside with skeletal texture in mela-quartz monzonite (sample 75–44) and from the pyroxene hornblendite enclave (sample 76–516). Based on three samples, orthopyroxenes from the JLP are in the range En_{62-72}. Compositions of pyroxenes in granitoids and enclaves are comparable (Fig. 9).

Discussion

Mineral assemblages and P_{H_2O}

Wones and Dodge (1977) and Wones (1981) concluded that, in the presence of quartz, magmas with moderate

Table 3. Representative analysis of rocks from the Abitibi Batholith, Jackfish Lake Pluton and the Otto Stock

	88-37	88-66	88-39	88-40	88-8	88-50	78-56	76-36	78-25	78-20	77-79	75-44	78-17	78-55	88-1108	88-99	88-120	88-103	88-104	88-114	78-7	88-1112
SiO_2	58.20	63.40	65.00	67.10	71.50	72.20	53.84	53.97	60.76	60.88	69.10	54.58	45.81	43.98	64.20	68.70	51.90	48.60	46.10	43.70	39.98	49.80
TiO_2	0.67	0.56	0.47	0.44	0.14	0.08	0.61	0.79	0.58	0.42	0.26	0.54	1.21	1.38	0.11	0.09	0.86	0.98	0.85	1.52	0.46	0.66
Al_2O_3	15.80	16.90	17.50	16.10	15.90	16.20	15.80	16.00	15.70	17.76	16.13	6.61	8.96	7.42	16.90	15.90	12.20	11.20	8.16	8.58	5.57	12.60
Fe_2O_3	1.26	1.76	1.24	0.94	0.53	0.30	1.74	2.57	2.36	1.42	0.94	2.78	4.29	4.57	1.65	0.84	4.39	2.91	3.29	5.50	6.00	2.28
FeO	5.59	2.86	2.60	2.73	0.40	0.67	5.68	4.69	2.96	2.22	1.04	5.33	7.55	8.46	0.60	0.47	4.39	7.19	6.85	9.32	5.61	5.31
MnO	0.11	0.07	0.05	0.05	0.05	0.02	0.14	0.16	0.07	0.03	0.03	0.18	0.20	0.20	0.04	0.03	0.18	0.19	0.17	0.18	0.19	0.15
MgO	5.50	2.00	1.66	1.38	0.34	0.33	6.56	5.72	3.70	2.45	0.95	10.62	13.16	14.74	0.97	0.61	4.78	10.50	14.30	14.60	23.44	7.87
CaO	6.61	5.26	4.80	4.13	1.84	2.58	8.08	7.79	5.44	4.26	1.94	13.78	13.21	13.74	1.75	0.80	8.12	10.60	12.00	11.40	7.44	7.60
Na_2O	3.26	4.41	4.64	3.99	6.28	4.71	4.73	4.86	4.76	6.64	5.18	1.76	1.93	1.92	7.04	6.26	2.22	2.82	1.80	1.49	0.41	5.44
K_2O	0.81	1.15	0.85	1.01	1.27	1.40	1.20	1.48	2.74	2.66	3.36	1.46	0.97	0.63	5.06	4.41	6.50	2.20	2.60	0.63	0.70	3.04
P_2O_5	0.15	0.14	0.10	0.10	0.04	0.04	0.54	0.46	0.27	0.19	0.09	0.52	0.78	0.98	00.00	0.02	1.03	0.36	0.37	0.03	0.38	0.50
CO_2	0.13	0.26	0.11	0.09	0.05	0.09	–	–	–	–	–	–	–	–	0.08	0.18	0.26	0.08	0.11	0.55	–	3.09
S	0.02	0.01	0.01	0.05	0.01	0.01	–	–	–	–	–	–	–	–	0.01	0.01	0.03	0.03	0.13	0.22	–	0.21
H_2O^+	1.64	1.07	0.98	1.16	0.27	0.72	–	–	–	–	–	–	–	–	0.18	0.16	1.00	1.33	1.52	2.33	–	1.61
H_2O^-	0.13	0.05	0.07	00.00	00.00	0.08	–	–	–	–	–	–	–	–	00.00	00.00	0.14	0.12	0.06	0.11	–	00.00
LOI	–	–	–	–	–	–	0.66	1.10	0.74	0.62	0.89	1.28	1.47	1.20	–	–	–	–	–	–	7.40	–
Total	99.90	99.90	100.10	99.30	98.60	99.40	99.58	99.61	100.08	99.55	99.91	99.44	99.54	99.23	98.60	98.50	98.00	99.10	98.40	100.10	97.58	100.10
Cr	151	24	26	25	11	10	275	143	98	84	19	420	565	670	45	19	69	515	1045	595	–	394
Ni	139	15	21	14	ND	ND	98	55	38	30	9	142	205	250	25	12	24	114	212	32	–	75
Sr	230	405	363	296	551	330	1472	1414	1060	1539	1070	204	316	322	336	371	2616	1045	512	342	246	1063
Zr	130	125	116	119	92	94	38	139	125	190	144	54	111	59	48	118	90	120	114	72	87	157
Y	19	13	10	9	5	6	12	16	9	8	3	23	28	28	7	8	36	25	20	23	9	25
Rb	24	28	28	32	26	38	17	26	65	28	81	44	13	8	59	110	151	68	100	14	26	110
La	–	12.60	11.10	16.60	2.46	4.77	50.00	46.00	44.00	33.00	20.00	37.00	36.00	40.00	6.03	10.30	190.00	22.50	33.20	5.38	21.80	60.0
Ce	–	29.00	22.20	32.60	5.98	10.40	110.00	115.00	91.00	77.00	49.00	110.00	115.00	120.00	15.90	22.60	417.00	56.70	82.20	16.60	54.30	130.0
Pr	–	3.85	2.64	3.54	0.810	1.24	13.00	14.00	10.00	9.00	4.20	15.00	17.00	18.00	2.12	2.44	50.40	8.05	11.40	3.00	7.01	16.0
Nd	–	15.60	9.64	12.10	3.10	4.52	57.00	61.00	43.00	38.00	16.00	69.00	85.00	89.00	8.08	8.25	192.00	35.30	51.30	15.50	27.70	11.0
Sm	–	3.14	1.86	2.24	0.674	0.816	9.50	11.00	7.30	6.40	2.30	13.00	17.00	18.00	1.69	1.53	32.50	7.57	10.10	4.41	4.73	61.0
Eu	–	0.967	0.654	0.688	0.184	0.220	2.70	2.60	2.00	1,70	0.67	2.80	3.30	4.20	0.362	0.380	7.47	2.05	2.43	1.32	1.20	2.7
Gd	–	2.47	1.44	1.61	0.534	0.603	6.50	7.00	4.60	4.00	1.40	8.50	11.00	13.00	1.11	1.10	19.90	6.27	7.42	4.54	3.09	8.3
Tb	–	0.313	0.185	0.218	0.56	0.54	0.68	0.79	0.48	0.45	0.16	0.95	1.30	1.40	0.127	0.128	2.05	0.786	0.790	0.628	0.34	0.940
Dy	–	1.77	1.07	1.25	0.278	0.335	3.20	3.60	2.40	2.00	0.84	4.70	6.50	6.30	0.707	0.823	9.63	4.56	4.38	4.20	1.86	5.1
Ho	–	0.322	0.197	0.228	0.54	0.49	0.53	0.62	0.38	0.35	0.13	0.82	1.10	1.10	0.115	0.160	1.43	0.828	0.722	0.755	0.30	0.870
Er	–	0.953	0.505	0.621	0.134	0.157	1.20	1.50	0.94	0.92	0.37	2.00	2.70	2.60	0.317	0.522	3.18	2.25	1.84	2.00	0.82	2.3
Tm	–	0.119	0.68	0.89	0.12	ND	0.18	0.21	0.12	0.12	0.05	0.27	0.35	0.31	0.39	0.69	0.349	0.302	0.223	0.251	0.10	0.300
Yb	–	0.806	0.466	0.529	0.120	0.114	1.00	1.30	0.69	0.73	0.38	1.80	2.00	1.80	0.335	0.595	2.22	1.90	1.42	1.55	0.59	2.0
Lu	–	0.104	0.054	0.063	0.012	ND	0.15	0.18	0.10	0.11	0.06	0.28	0.28	0.27	0.045	0.085	0.345	0.257	0.208	0.216	0.08	0.300
Mg′	0.681	0.471	0.469	0.433	0.434	0.410	0.642	0.618	0.590	0.581	0.499	0.729	0.695	0.699	0.480	0.496	0.532	0.679	0.743	0.670	0.808	0.679
Al′	0.865	0.936	1.013	1.062	1.056	1.161	0.665	0.673	0.759	0.824	1.028	0.224	0.317	0.257	0.580	0.962	0.479	0.426	0.296	0.360	0.372	0.484
Mol Na/K	6.117	5.829	8.297	6.004	7.516	5.113	5.991	4.991	2.640	3.794	2.343	1.832	3.024	4.632	2.115	2.158	0.519	1.948	1.052	3.595	0.890	2.720
Ce_N/Yb_N	–	8.18	10.83	14.01	11.33	20.73	25.00	20.10	29.97	23.97	29.31	13.89	13.07	15.15	10.79	8.63	42.69	6.78	13.16	2.43	20.92	14.81
Eu/Eu*	–	1.03	1.2	1.1	0.9	0.9	0.97	0.85	0.97	0.96	1.06	0.76	0.69	0.80	0.69	0.83	0.83	1.13	1.21	1.11	0.902	0.81
Rb/Sr	0.104	0.069	0.077	0.108	0.047	0.115	0.011	0.018	0.061	0.018	0.076	0.216	0.041	0.025	0.175	0.296	0.058	0.065	0.195	0.041	0.106	0.103
K/Rb	280	341	252	262	405	306	586	472	350	789	344	275	619	654	712	333	357	269	216	373	223	229

ND – not detected; – not determined; FeO determined by wet chemical methods: Mg′ = mol MgO/(MgO + 0.9 FeO^t); Al′ = mol Al_2O_3/(CaO + Na_2O + K_2O); Ce_N/Yb_N = chondrite normalized ratio Ce/Yb; Eu* = hypothetical value of Eu based on interpolation between Sm and Gd. Samples are identified in Table 1.

Table 4. Average analyses of granitoid Rocks from Lac des Iles, Abitibi Batholith, Jackfish Lake Pluton and the Otto Syenite

Wt %	Lac des Iles Tonalite n = 8	Abitibi Tonalite n = 15	Jackfish Lake Diorite n = 5	Jackfish Lake Monzodiorite n = 11
SiO_2	68.90 (63.36–72.39)	68.64 (61.68–74.81)	55.47 (54.42–57.08)	61.99 (58.99–65.55)
TiO_2	0.42 (0.33–0.55)	0.34 (0.08–0.57)	0.67 (0.59–0.80)	0.55 (0.39–0.65)
Al_2O_3	16.24 (15.36–18.07)	16.35 (14.72–17.79)	15.36 (12.67–16.96)	15.99 (15.14–17.95)
Fe_2O_3	1.15 (0.64–2.05)	1.13 (0.30–2.06)	2.29 (1.76–2.61)	1.98 (1.44–2.59)
FeO	2.27 (1.63–2.93)	1.98 (0.41–3.33)	4.75 (4.17–5.74)	2.92 (1.92–3.78)
MnO	0.05 (0.03–0.08)	0.04 (0.01–0.09)	0.13 (0.11–0.16)	0.07 (0.02–0.10)
MgO	1.39 (0.82–2.08)	1.49 (0.32–3.62)	6.65 (5.81–8.27)	3.66 (2.20–4.61)
CaO	4.41 (3.63–5.49)	3.92 (1.87–5.34)	8.01 (6.97–8.76)	4.94 (3.34–6.30)
Na_2O	3.92 (3.65–4.28)	4.91 (3.75–6.58)	4.52 (3.84–4.94)	4.71 (4.14–6.71)
K_2O	1.13 (0.82–1.71)	1.08 (0.27–1.86)	1.71 (0.90–2.74)	2.92 (2.29–3.63)
P_2O_5	0.09 (0.07–0.13)	0.09 (0.02–0.19)	0.42 (0.32–0.55)	0.26 (0.14–0.37)
Ni	12 (5–19)	16 (ND-55)	76 (55–99)^2	34 (30–38)^2
Cr	28 (12–52)	27 (6–110)	209 (143–275)^2	91 (84–98)^2
Rb	28 (12–49)	28 (13–48)	30 (11–51)	69 (28–112)^7
Sr	273 (241–340)^7	395 (213–706)	1375 (1206–1509)	1095 (717–1539)^7
Zr	150 (136–170)^6	131 (78–244)	79 (38–139)	174 (125–218)^7
Y	9 (5–15)	10 (5–13)	13 (10–16)	10 (6–13)^7
Ce	32 (19–38)^4	20 (6–33)^5	112 (110–115)^2	84 (77–91)^2
Yb	0.60 (0.25–0.86)^4	0.41 (0.11–0.81)^5	1.15 (1.00–1.30)^2	0.71 (0.69–0.73)^2
Mg′	0.45 (0.40–0.48)	0.46 (0.23–0.64)	0.66 (0.62–0.73)	0.60 (0.58–0.63)
Al′	1.04 (0.96–1.12)	1.01 (0.80–1.18)	0.65 (0.50–0.72)	0.81 (0.74–0.89)
Mol·Na_2O/K_2O	5.52 (3.80–7.96)	8.70 (3.36–29.38)	4.83 (2.13–8.03)	2.49 (1.88–3.78)
Ce/Yb_n	13 (8–17)	3 (8–21)	23 (20–25)	27 (24–30)
Eu/Eu^*_n	1.2 (0.9–1.9)	1.0 (0.9–1.2)	0.9 (0.8–1.0)	1.0 (1.0–1.0)
Rb/Sr	0.101 (0.048–0.144)	0.075 (0.035–0.115)	0.023 (0.007–0.042)	0.068 (0.018–0.156)
K/Rb	352 (282–556)	302 (174–407)	516 (356–666)	428 (248–796)

Superscripted numbers for trace elements indicate number of analyses; numbers in brackets indicate ranges

K_2O crystallize clinopyroxene + biotite at low P_{H_2O}, while at higher P_{H_2O}, amphibole crystallizes before biotite. This suggests that the occurrence of biotite – augite diorite in the JLP reflects lower P_{H_2O} during crystallization than the biotite – hornblende diorite in the JLP. The pyroxene – dominated assemblages of OS also indicate relatively low P_{H_2O} during crystallization of this intrusion. These assemblages contrast with the biotite-hornblende assemblages in the AB and LDI tonalites.

Microcline is the predominant alkali feldspar in the AB, LDI, and JLP. The microcline is late and partially replaces plagioclase locally. Longstaffe et al. (1980) have provided petrographic and geochemical evidence for autometasomatic growth of microcline megacrysts in granodioritic rocks of the JLP. Similar textures are observed in monzonitic rocks of the JLP and microcline megacrystic phases of the OS. In contrast to the other hornblende – bearing suites, alkali granite of the OS contains perthite with typical hypersolvus texture indicative of crystallization at low P_{H_2O} (Tuttle and Bowen 1958; Morse 1970). In summary, mafic mineral assemblages and feldspar textures indicate that, with increasing alkalis and decreasing silica-saturation, the examined plutons record crystallization at lower P_{H_2O}. This correlation suggests that the mineral assemblages reveal information on the original water content of the magma.

Evidence for amphibole fractionation

Mela-granitoids and mafic-ultramafic units associated with the LDI tonalites, JLP monzodioritic suite and OS syenite have similar textural and geochemical characteristics. The texture of these rocks with abundant, coarse, euhedral, and often skeletal amphibole or pyroxene with interstitial felsic minerals suggests that the mafic minerals are cumulus phases. Analyzed hornblende separates from AB, LDI, and JLP have similar REE abundances to the majority of mela-granitoids and mafic-ultramafic units (Fig. 8). Even if the hornblende separates contained included a small amount of accessory minerals such as apatite, the analyzed separate may still be representative of the cumulus fraction. Higher total REE in hornblende separates than in some associated melanocratic phases (eg. LDI sample 85–234) reflects the presence of significant quartz and feldspar in these melanocratic units. Comparable X_{Mg} in pyroxenes and amphiboles from ultramafic enclaves and dioritic rocks of the JLP and amphibole-rich igneous layers in syenite of the OS are consistent with the cumulate model. A similar origin for hornblendite has been proposed by Arth et al. (1978) in a suite of Proterozoic tonalites in Finland and by Bender et al. (1984) in amphibole-bearing mafic and ultramafic alkaline rocks of the Cortlandt Complex.

Skeletal hornblende in LDI mela-tonalite (85–234) has higher X_{Mg} than the adjacent host granitoids (Fig. 9). The REE abundances of this rock are similar to other ultramafic enclaves and suggest that, despite the skeletal textures, this phase is an ortho-cumulate derived from a liquid with higher Mg′ than the granitoid host.

In the granitoid rocks, fractionation of amphibole explains the negative correlation of elements such as CaO, MgO, FeO, TiO_2, Ni and Cr with SiO_2, the rapid

Jackfish Lake Monzonite n=4	Otto Syenite n=5
64.02 (60.39–69.78)	66.69 (63.81–70.04)
0.42 (0.26–0.55)	0.17 (0.09–0.29)
16.42 (15.99–17.03)	17.01 (15.83–18.04)
1.60 (0.95–2.08)	1.41 (0.86–1.76)
2.18 (1.05–3.23)	0.73 (0.48–1.08)
0.07 (0.03–0.10)	0.04 (0.03–0.05)
2.46 (0.96–4.39)	0.84 (0.56–1.07)
3.51 (1.96–5.40)	1.41 (0.82–1.86)
4.96 (4.51–5.23)	6.62 (6.37–7.16)
4.11 (3.21–5.30)	5.02 (4.48–5.55)
0.24 (0.09–0.33)	0.06 (0.00–0.11)
9 (9)[1]	13 (7–25)
19 (19)[1]	26 (17–45)
106 (43–195)[3]	93 (59–130)
639 (253–1127)	
266 (143–511)[3]	147 (48–250)
6 (3–9)[2]	21 (7–38)
49 (49)[1]	19 (16–23)[2]
0.38 (0.38)[1]	0.47 (0.34–0.60)[2]
0.53 (0.47–0.60)	0.46 (0.42–0.50)
0.87 (0.77–1.03)	0.90 (0.83–0.96)
1.90 (1.46–2.34)	2.02 (1.80–2.16)
29 (29)[1]	10 (9–11)
1.1 (1.1)[1]	0.8 (0.7–0.8)
0.098 (0.034–0.183)	0.197 (0.076–0.324)
398 (226–621)	473 (332–714)

initial depletion of MgO, Ni and Cr, and the positive correlation of elements such as Rb, K and Zr with SiO_2. Note that Rb, K_2O, and Zr decrease with increasing SiO_2 at LDI and this exception is consistent with the role of magma mixing (Sutcliffe 1989). Variation of Al_2O_3 with SiO_2 indicates that a phase more aluminous than the observed amphiboles must be involved in the fractionation.

Amphibole is present in some enclaves and mafic rocks with higher Al than in the granitoids, e.g., kaersutite in sample 88–104, hornblende in sample 76–516. This suggests that fractionation of aluminous amphiboles at higher pressure than that at which the granitoids crystallized is a posible explanation of the required aluminous phase. Hammarstrom and Zen (1986) indicate that amphiboles crystallizing from calc-alkaline magmas at 6–10 kbar will contain approximately 2.2 Al ions per amphibole formula unit. This composition is exceeded by several amphiboles of the mafic core of the OS and approached by amphiboles in enclaves of the JLP. Plagioclase fractionation is also a probable factor as indicated, for example, by the slight decrease in Sr with increasing SiO_2 in the JLP. The role of plagioclase fractionation, however, is considered to be subordinate to amphibole for several reasons. Firstly, negative Eu anomalies and significantly lower Sr are not observed in the more fractionated rocks. Secondly, in rocks with petrographic and geochemical characteristics of a cumulus origin, plagioclase is not observed as a significant phase. Finally, experimental studies of hydrous andesitic compositions indicate that at 8–12 kbar amphibole is the dominant crystallizing phase and that plagioclase is not a liquidus phase above 5 kbar (Wyllie 1977; Green 1982).

High concentrations of apatite in some melanocratic phases and the generally high but irregular abundance of P_2O_5 in these rocks indicates that apatite is also a probable cumulus mineral.

Major, trace and rare earth element characteristics of the fractionated rocks in each suite are generally consistent with an origin as differentiates in a system dominated by amphibole fractionation. Least-squares mass-balance calculations using XLFRAC (Stormer and Nicholls 1978) indicate that an acceptable model (based on all major oxides except MnO and using FeO^t) for deriving the average JLP monzonite from the average JLP diorite (Table 4) may be obtained by subtracting hornblende (analysis 10, table 5), plagioclase (An_{23}), and apatite and the proportions 62.2:36.2:1.5. This model requires that the subtracted phases are equivalent to 66% of the initial magma and produces a solution in which the square of the sum of the residuals is 1.35.

In the JLP and the other suites, decreasing HREE and Y with increasing SiO_2 support the role of amphibole fractionation (Frey et al. 1978). Longstaffe et al. (1980, 1982) demonstrated that model REE patterns for 10 to 20% hornblende fractionation of a melt of dioritic composition are similar to observed REE patterns of fractionated rocks of the JLP. HREE variation in LDI tonalites, AB tonalites, OS syenites and LDI dikes can be attributed to 10–30% fractionation of amphibole assuming that granitoids with the lowest SiO_2 and highest Mg′, Cr, and Ni in each suite are representative of initial liquid compositions (Fig. 10 and Sutcliffe 1989, Fig. 9). Furthermore, REE in the JLP, LDI and some OS (e.g. 88–114) mela-granitoids and mafic-ultramafic units can be modelled as cumulates from initial liquids with fractionated REE abundances comparable to the most primitive granitoid rocks in the respective suites (Figs. 9 and 10).

The effect of addition of plagioclase to the amphibole fractionation model is to suppress the formation of a positive Eu anomaly in the granitoids and to allow for greater degrees of fractionation. The addition of 1.5% apatite increases the bulk distribution coefficient of the fractionated assemblage but does not significantly change the profile of the amphibole–dominated bulk distribution coefficient. An amphibole–plagioclase–apatite fractionation model for the JLP is given in Fig. 10c.

The REE and Y data for the suites are also compatible with fractional melting models involving amphibole, however, the fractional crystallization model is preferred due to the recognition of in-situ amphibole-rich cumulate layers and other amphibole-rich cumulate units which occur in proportions that account for much of the cumulus material required by this model. Hornblende and clinopyroxene are silica undersaturated relative to the parental magmas, and fractionation of these minerals results in silica-oversaturated residual liquids, as noted by Shirey and Hanson (1984). Similarly, amphibole fractionation results in residual liquids having higher $Al_2O_3/(Na_2O+K_2O+CaO)$ than initial liquids (Zen 1986).

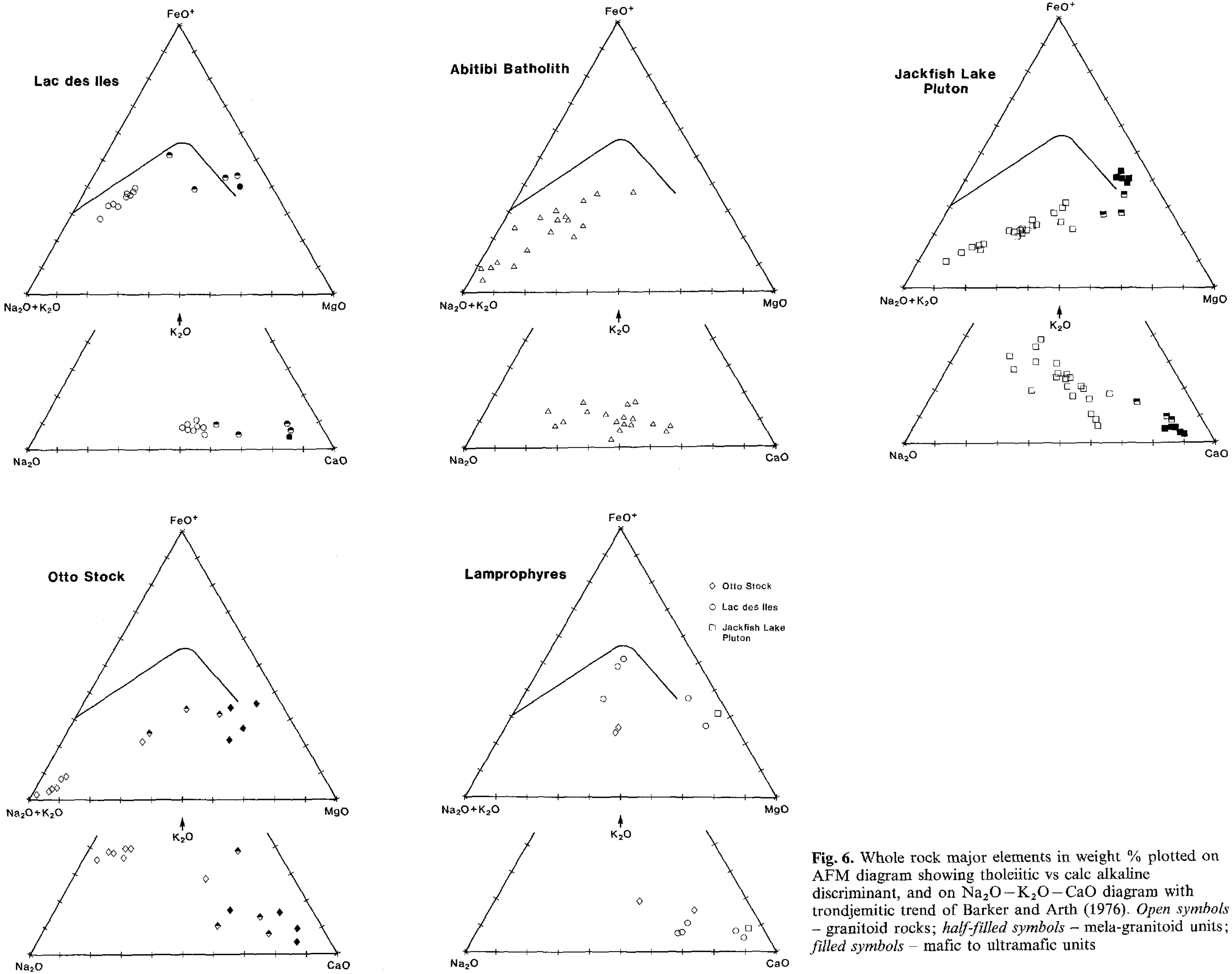

Fig. 6. Whole rock major elements in weight % plotted on AFM diagram showing tholeiitic vs calc alkaline discriminant, and on Na_2O-K_2O-CaO diagram with trondjemitic trend of Barker and Arth (1976). *Open symbols* – granitoid rocks; *half-filled symbols* – mela-granitoid units; *filled symbols* – mafic to ultramafic units

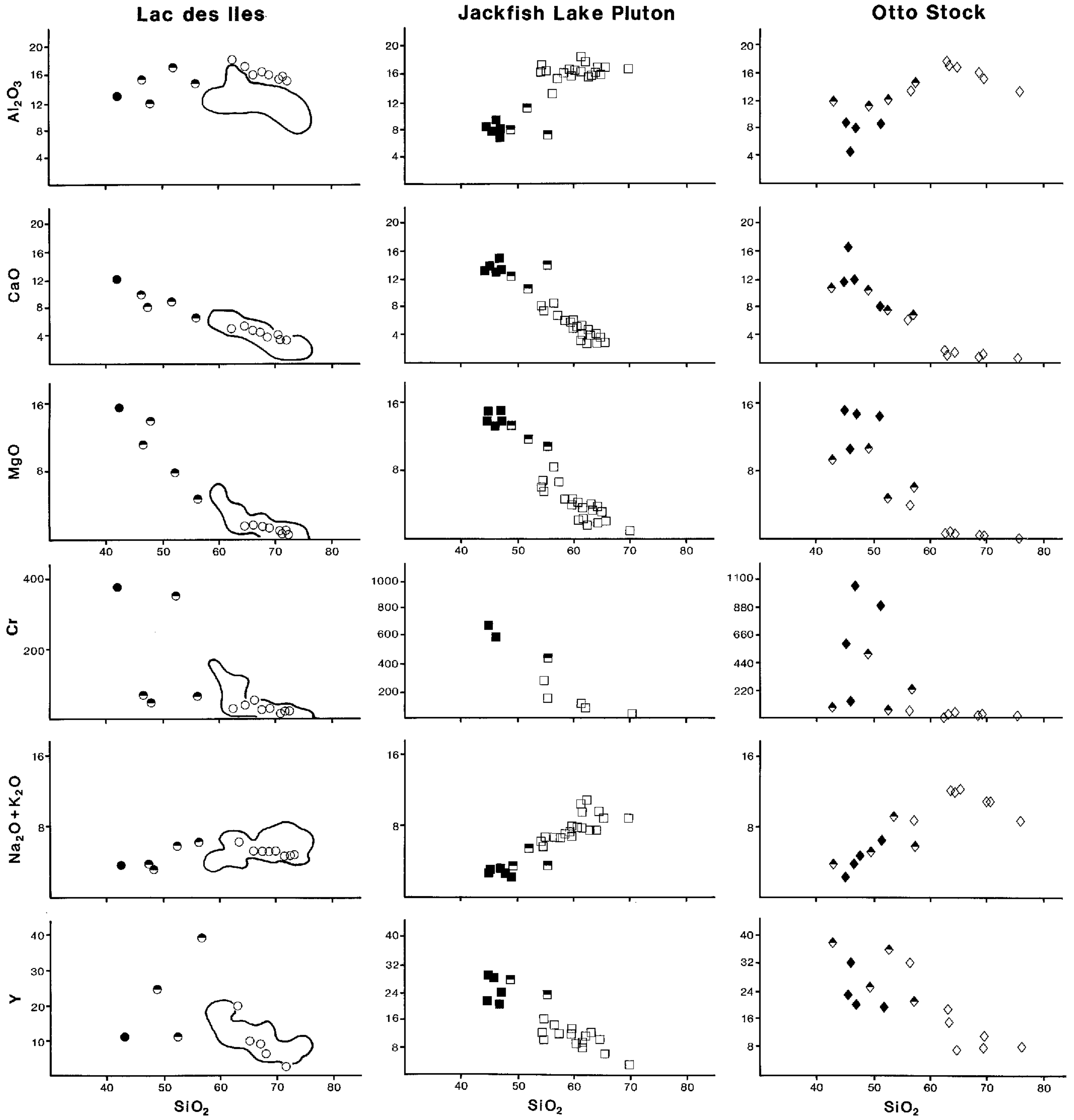

Fig. 7. Harker variation diagrams for Al_2O_3, MgO, CaO, Na_2O+K_2O (weight % recalculated on an anhydrous basis), Cr, and Y (ppm). Symbols as in **Fig. 6**: *open* – granitoid rocks; *half-filled* – mela-granitoid units; *filled* – mafic to ultramafic units. Fields for Abitibi Batholith data are given with Lac des Iles

With the exception of aegirine–augite in pyroxenites of OS, amphibole is the dominant constituent of all of the mafic to ultramafic units in the intrusions studied, even where the granitoids contain pyroxene+biotite. The presence of amphibole in these rocks may be due to the crystallization and accumulation of amphibole at higher pressures and in the absence of feldspar and quartz. A discrepancy between the model REE patterns in Fig. 10 and the observed patterns is that decreasing LREE are also observed with increasing SiO_2. A possible explanation of this may be the effect of dilution by accumulation of microcline in the more fractionated granitoids.

Lamprophyre dikes have REE compositions intermediate between granitoid and cumulate phases at LDI (Fig. 8). Based on REE abundances, the LDI tonalites

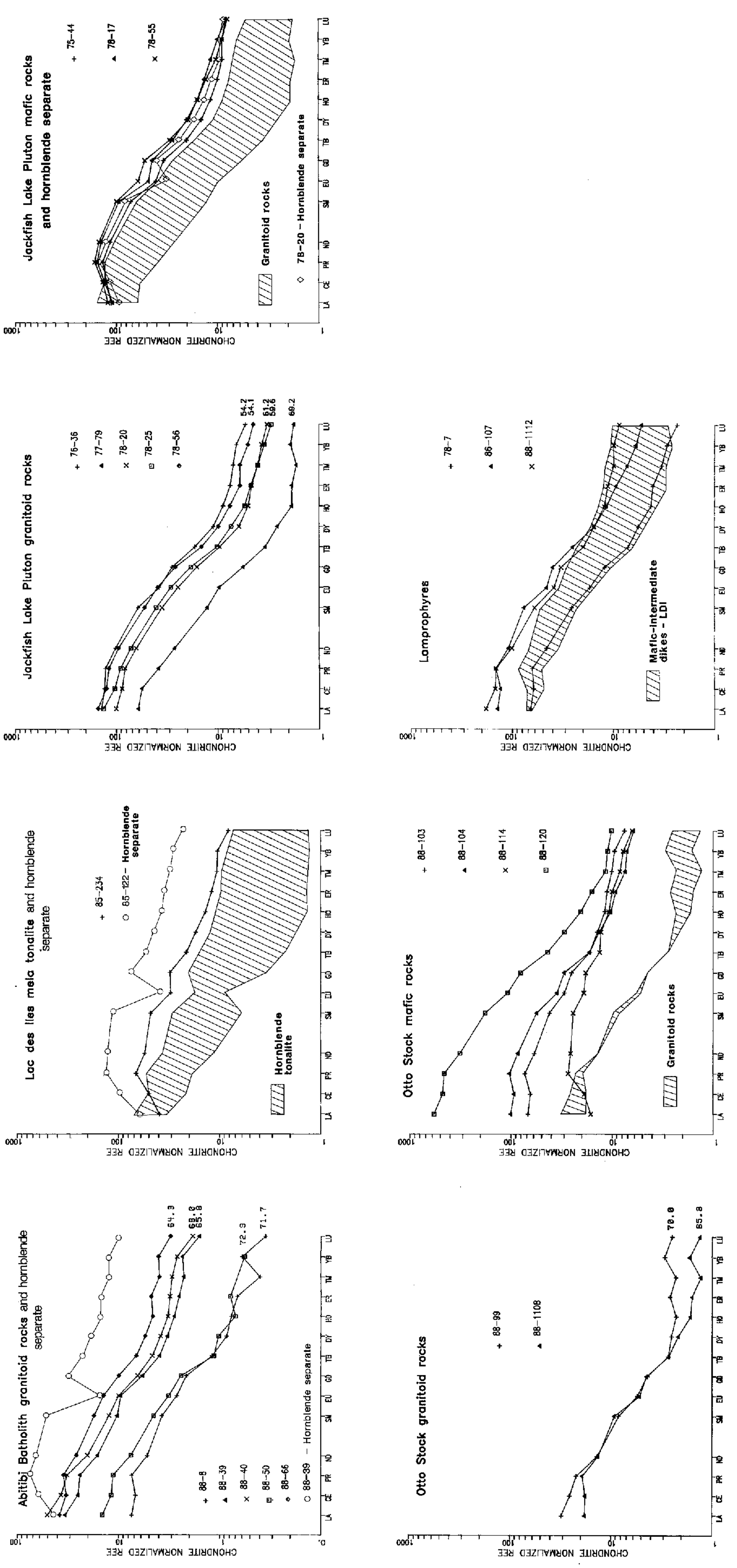

Fig. 8. Chondrite normalized REE profiles for granitoids, associated mafic rocks, and hornblende separates. Chondrite normalizing values from Haskin et al. (1968). *Numbers at right* of REE profiles for granitoids are wt% SiO_2. Analyses from the **LDI** area from Sutcliffe (1989)

Table 5. Representative analyses of pyroxenes and amphiboles from the Abitibi Batholith, Otto Stock and Jackfish Lake Pluton

	Pyroxenes							Amphiboles							
	1	2	3	4	5	6		7	8	9	10	11	12	13	14
SiO_2	53.54	52.26	51.79	51.88	55.26	53.52	SiO_2	47.28	53.68	46.00	43.84	39.98	48.20	42.98	51.32
TiO_2	0.07	0.16	0.03	0.25	–	0.04	TiO_2	0.76	0.00	0.54	2.18	5.73	0.73	1.87	0.39
Al_2O_3	0.75	0.55	0.84	2.07	0.71	0.46	Al_2O_3	6.04	2.12	8.03	9.83	13.72	6.44	10.17	2.14
Fe_2O_3	2.88	14.02	2.63	4.35	–	–	Fe_2O_3	4.65	–	–	2.35	1.10	1.11	3.78	0.82
Cr_2O_3	0.00	0.00	0.00	0.00	–	0.00	FeO	15.20	13.13	17.33	8.97	11.21	9.30	8.02	14.12
FeO	4.19	5.79	5.16	4.31	18.68	8.24	MnO	0.35	0.29	0.27	0.06	0.16	0.14	0.05	0.53
MnO	0.22	0.48	0.25	0.18	0.52	0.44	MgO	11.13	17.16	12.56	15.07	11.62	16.49	14.83	14.48
MgO	14.70	7.17	13.59	14.87	26.82	13.04	CaO	11.78	11.59	10.74	11.83	9.80	11.63	11.31	7.23
CaO	23.41	15.25	22.51	21.87	0.56	23.96	Na_2O	1.02	–	–	2.13	3.11	2.85	2.26	4.54
Na_2O	0.75	5.23	0.75	0.70	–	–	K_2O	0.41	0.20	0.97	1.07	1.66	0.55	0.84	0.89
Total	100.51	100.90	97.55	100.49	102.55	99.70	Total	98.63	98.23	96.46	97.32	98.09	97.43	96.11	96.46
Si	1.969	1.973	1.970	1.913	1.969	2.004	Si	7.011	7.700	6.933	6.446	5.914	7.009	6.389	7.640
Al^{IV}	0.031	0.024	0.030	0.087	0.030	0.002	Al^{IV}	0.989	0.359	1.426	1.554	2.086	0.991	1.611	0.360
Al^{VI}	0.001	0.000	0.008	0.003	0.030	0.002	Al^{VI}	0.067	–	–	0.150	0.306	0.112	0.172	0.016
Fe^{2+}	0.129	0.183	0.164	0.133	0.557	0.258	Fe^{2+}	1.886	1.575	2.185	1.103	1.386	1.130	0.997	1.758
Fe^{3+}	0.080	0.398	0.075	0.121	–	–	Fe^{3+}	0.519	–	–	0.260	0.123	0.121	0.423	0.092
Mg	0.806	0.403	0.771	0.817	1.424	0.727	Mg	2.460	3.668	2.821	3.302	2.562	3.573	3.286	3.213
Mn	0.007	0.015	0.008	0.006	0.016	0.014	Mn	0.044	0.035	0.034	0.008	0.020	0.017	0.006	0.067
Ti	0.002	0.005	0.001	0.007	–	–	Ti	0.085	0.000	0.061	0.241	0.637	0.080	0.209	0.044
Cr	0.000	0.000	0.000	0.000	–	–	Ca	1.872	1.782	1.734	1.864	1.553	1.812	1.802	1.153
Ca	0.922	0.617	0.918	0.864	0.021	0.961	Na	0.293	–	–	0.607	0.892	0.804	0.651	1.310
Na	0.053	0.383	0.055	0.050	–	–	K	0.078	0.036	0.187	0.201	0.313	0.102	0.159	0.169

1 = Augite, pyroxene – hornblendite, OS (88–104/2B)
2 = Aegerine – augite, alkali granite, OS (88-99/1A)
3 = Augite, skeletal, mela-monzonite, JLP (74-44/1B)
4 = Augite, pyroxene – hornblendite enclave, JLP (76-516/1A)
5 = Hypersthene, pyroxene – hornblendite enclave, JLP (76-516/1-1)
6 = Augite, hornblende monzodiorite, JLP (76-8/4-2)
7 = Hornblende, tonalite, AB (88-40/1A)
8 = Actinolite, rims cpx, monzodiorite, JLP (76-25/3-1)
9 = Hornblende, rims actinolite, JLP (76-25/3-3)
10 = Hastingsitic hornblende, opx – cpx – hornblendite, JLP (16-516/3)
11 = Kaersutite, core, pyroxene-amphibolite, OS (88-104/1A)
12 = Edenite, rim, pyroxene – amphibolite, OS (88-104/3B)
13 = Hastingsitic hornblende, core, hornblende cumulate layer, OS (88-116/2A)
14 = Silicic edenite, alkali granite, OS (88-99/1A)

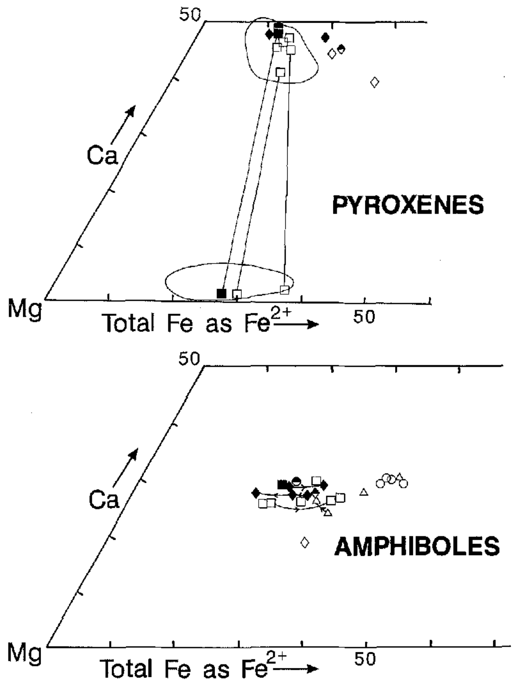

Fig. 9. Amphiboles and pyroxenes plotted in atomic proportions. Analyses represent rock averages except for some amphiboles where substantial core to rim variation is indicated by *lines with arrow*. Coexisting augite and hypersthene compositions are indicated by *tie-lines*. *Outlined* are fields of pyroxenes from the mafic to ultramafic Lac des Iles Complex (Sutcliffe et al. 1989). *Symbols* as in **Fig. 6**

Table 6. Trace element analyses of hornblende separates

ppm	1	2	3
Rb	4	1	2
Y	68	31	24
La	20.3	14.9	31.8
Ce	86.0	56.3	107
Pr	14.6	9.04	16.7
Nd	75.3	40.8	76.0
Sm	20.1	9.63	14.6
Eu	2.62	1.02	2.16
Gd	18.8	7.97	10.2
Tb	2.46	1.09	1.12
Dy	14.2	6.14	5.46
Ho	2.62	1.07	0.90
Er	6.98	3.03	2.31
Tm	0.90	0.38	0.30
Yb	5.80	2.57	1.84
Lu	0.77	0.35	0.28
CeN/YbN	3.37	4.98	13.2
Eu/Eu*	0.41	0.35	0.51

1 = Hornblende from tonalite, *LDI* (85-122, see Sutcliffe 1989 for analysis
2 = Hornblende from tonalite, AB (88-39)
3 = Hornblende from monzodiorite, *JLP* (78-20)

could be modelled as derived from the dikes by amphibole fractionation (Sutcliffe 1989). We suggest, however, that because the lamprophyre dikes are commonly observed to intrude the granitoids, the dikes are best considered as cogenetic (but not necessarily comagmatic) mafic components of the plutons.

Evidence for magma mixing

At Lac des Iles, textures such as net-veined dike rocks, mafic dike swarms, mafic schlieren, skeletal hornblende in mela-tonalite, and resorbed hornblende in tonalite suggest that mixing between mafic and tonalitic magmas took place (Sutcliffe 1989). These textures are similar to those reported in Phanerozoic granitic rocks where magma mixing has been documented (e.g. Reid et al. 1983; Furman and Spera 1985; Hyndman and Foster 1988).

Features suggestive of contemporaneous mafic and felsic magmatism, such as hornblendite to microdiorite enclaves with rounded or cuspate surfaces, are present in all of the plutons in this study. Another feature observed in LDI, MLP, and OS is skeletal hornblende or augite in the melanocratic granitoid phases. The origin of the mela-quartz monzonite (JLP) and mela-syenite

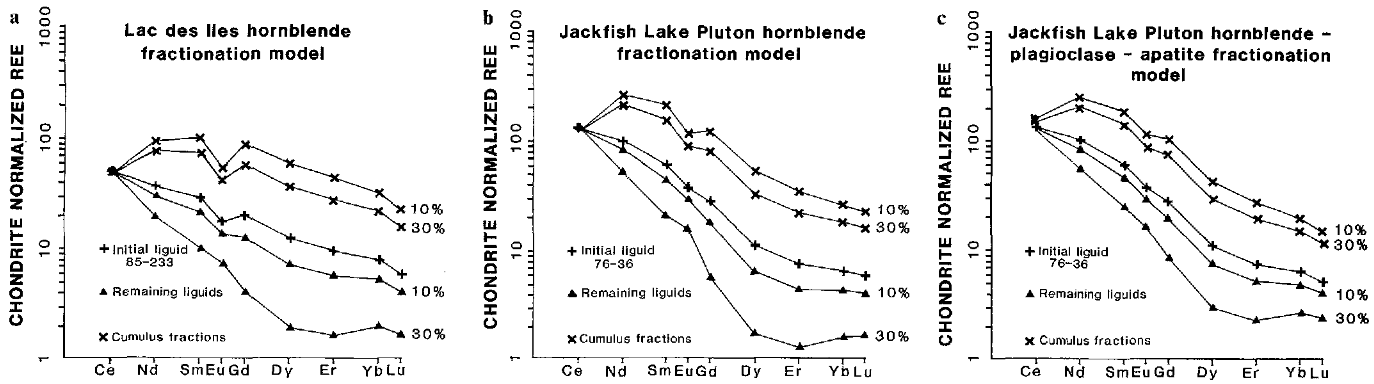

Fig. 10. REE fractionation models for granitoid suites. Models **a** and **b** based on hornblende partition coefficients for intermediate liquids (Arth 1976). Model **c** based on hornblende and plagioclase partition coefficients in intermediate liquids and apatite in felsic liquid from Arth (1976). Fractionated assemblage of 62.5% amphibole, 36.0% plagioclase and 1.5% apatite in model **c** is based on the major element mass balance calculation. All models assume perfect fractional crystallization. Initial liquid compositions, based on the most primitive granitoid in the suites are from table 3 and Sutcliffe (1989, Fig. 6)

(OS) may be similar to that of mela-tonalite in LDI tonalite where skeletal amphiboles are associated with injection of mafic magma into tonalitic magma (Sutcliffe 1989). The skeletal textures are attributed to supercooling of the mafic phase during mixing with a felsic phase. This process is also described in some volcanic suites (Gerlach and Grove 1982; McMillan and Dungan 1986). The skeletal pyroxene and amphibole show that the mafic minerals are unlikely to be restite.

Sutcliffe (1989) reported that approximately 20% of the outcrops of LDI hornblende tonalite have evidence of magma mixing and that geochemical variation in the tonalite was consistent with mixing of tonalitic and mafic magmas. Other plutons considered in this study, however, do not show such extensive field evidence of mixing. We suggest that mixing of felsic and mafic magmas may control geochemical variation locally, but is subordinate to fractionation of amphibole. One significant aspect of mixing textures is that they provide evidence for contemporaneous mantle-derived mafic magmas.

Evidence for mantle origin

Longstaffe et al. (1980, 1982) proposed that dioritic to monzodioritic rocks of JLP are derived from melting of eclogite. This is similar to models of Arth and Hanson (1975) to produce the geochemically similar Vermilion District syenodiorites. Shirey and Hanson (1984) suggested that Archean monzodioritic rocks are derived from direct melting of LILE (such as Ba, Sr, LREE) enriched mantle sources at depths of <50 km under hydrous or anhydrous conditions. They include the JLP diorites as an example of rocks produced by this process.

Shirey and Hanson (1984) showed that primitive members of the monzodiorite suite have high Ni (180–200 ppm) and Cr contents compared with their Mg′ (0.60–0.64) which indicate that they could not have undergone extensive fractional crystallization. The most primitive members of the suite have compositions comparable to experimentally-derived liquids from mantle compositions and to mantle-derived high-Mg andesites (sanukites) (Shirey and Hanson 1984). Monzodioritic rocks of Rainy Lake area have ε_{Nd} values at 2.7 Ga of $+1.0$ to $+1.5$ (Shirey and Hanson 1986). The elevated light REE abundances in conjunction with depleted $^{143}Nd/^{144}Nd$ ratios suggest that the mantle source was enriched in LILE shortly before melting (Shirey and Hanson 1984). It is not possible to explain elevated abundances of Sr and LREE by crustal contamination because must Superior Province supracrustals and granitoids have lower abundances of these elements than the monzodiorites (Shirey and Hanson 1984). ε_{Nd} of $+1.0$ to $+2.2$ are also reported for late alkaline volcanic and intrusive rocks in the Abitibi Subprovince (Barrie and Shirey 1989; Basu et al. 1984), a suite to which the OS is considered to belong (Wyman and Kerrich 1988).

The OS syenitic rocks and the AB and LDI tonalitic rocks and associated melanocratic phases show similar geochemical characteristics to the JLP, particularly in abundances of REE, Cr, and Ni. The X_{Mg} of pyroxenes in mafic cumulates at the JLP and OS are comparable to pyroxenes in Late Archean mafic-ultramafic intrusions such as the Lac des Iles Complex (Sutcliffe et al. 1989) (Fig. 9). Similar conclusions apply to high X_{Mg} in amphiboles from the LDI, AB, JLP, and OS (Fig. 9). High abundances of Ni (generally >100 ppm) and Cr (>150 ppm) in primitive granitoid phases indicate that the liquids were not extensively fractionated. The Cr and Ni abundances are not compatible with models that require small degrees of melting of basaltic or eclogite sources to produce the fractionated REE.

The plutons examined in this study indicate that a range of late Archean granitoids from tonalite to syenite may be derived from the mantle by similar processes to those proposed by Shirey and Hanson (1984). In particular, most tonalitic rocks have previously been considered as part of the tonalite – trondhjemite – granodiorite suite and are generally considered to be derived by partial melting of amphibolite or eclogite (Martin 1986). Although a mantle-derivation is proposed, contamination of magmas by a crustal component, as suggested by some isotopic studies in the Abitibi Subprovince (e.g. Gariepy and Allegre 1985), it not precluded by the results reported here.

Further field evidence for the mantle origin of the suites is the presence of cogenetic lamprophyre dikes and mafic intrusions. Melagranitoids, particularly those with skeletal mafic minerals, provide evidence for a possible comagmatic link between lamprophyres and the granitoids. The consensus that calc-alkaline lamprophyre magmas are derived from LILE-enriched mantle soures (Rock and Groves 1988; Wyman and Kerrich 1989) is similar to the process proposed by Shirey and Hanson (1984) for monzodioritic rocks.

Comparison with modern volcanic arcs suggest that subduction of crustal material may account for the mantle-enrichment process (e.g. Ellam and Hawkesworth 1988) although alternatives are possible (e.g. Edgar 1983). A similar approach has been used by Wyman and Kerrich (1988, 1989) and Rock and Groves (1988) to suggest that sources of Archean lamprophyres may be a LILE-enriched mantle wedge and that these rocks may be related to the late stages of a subduction regime.

The association and distribution of gabbro, diorite, lamprophyres, and mela-granitoids with more voluminous felsic granitoids in these Archean suites is similar to some Phanerozoic subduction-related granitoid suites (e.g., western part of the Cordilleran Peninsula Ranges Batholith-Silver and Chappell 1988; Scottish Caledonian granites – Fowler 1988). The more mafic phases of the Archean suites are also similar to M-type granitoids formed in modern oceanic arc terrains (e.g. Uasilau Yau-Yau Complex of New Britain – Whalen 1985). These similarities suggest a similar origin for Archean suites in the Superior Province greenstone-granitoid terrains.

Role of volatiles

Experimental studies by Kushiro (1972) demonstrated that partial melting of garnet lherzolite in the presence of water produces quartz-normative melts to pressures of at least 25 kbar. At 20 kbar SiO_2- and Al_2O_3-rich liquids with compositions comparable to andesite-dacite are produced. With increased melting, liquid composition passes to the vapour absent region and melts become less silicic. Subsequently, Mysen and Boettcher (1975) determined that the silica saturation of liquids formed by anatexis of mantle peridotite varies with vapour composition. In the system peridotite-CO_2-H_2O, quartz normative andesitic liquids are produced by anatexis under $X_v^{H20} > 0.6$ to at least 25 kbar total P and to > 200° C above the peridotite solidus. Melts formed at $X_v^{H20} < 0.4$ are silica undersaturated and alkalinity of the melt increases with decreasing X_v^{H20}. Other experimental studies are consistent with a mantle-origin from silica-oversaturated melts at pressures < 5 kbar at temperatures of ~1,150–1,250° C in anhydrous conditions (Jaques and Green 1980; Mysen and Kushiro 1977; Presnall et al. 1979).

Shirey and Hanson (1984) noted that production of silica-oversaturated mantle-derived melts may have been common in the Archean given that a hotter mantle (Bickle 1978) may have allowed melting at shallow depths in a variety of tectonic settings. The presence of water during melting would promote silica oversaturation, conversely, if melting were dry or in the presence of CO_2, melts would have been silica undersaturated. Deeper melting would also produce less silica saturation.

Mineralogical evidence in the granitoid suites examined in this study indicates progressively lower P_{H_2O} with increasing alkalinity, Sr- and LREE-enrichment, and decreasing silica oversaturation. Corfu et al. (1989) have shown that the ages of plutonic rocks in the Abitibi Subprovince support a secular evolution from early (~2.70 Ga) tonalitic plutons to later (~2.67 Ga) syenitic plutons. Late Archean alkali-rich intrusive rocks such as OS have been implicated in magmatic genetic models for gold mineralization based on their close spatial and temporal association with gold mineralization (e.g., Wyman and Kerrich 1988) and oxidized nature (Cameron and Hattori 1987). Fyon et al. (1989) suggest that gold mineralization and alkaline magmatism may be a manifestation of the cratonization process resulting from the involvement of mantle melts and CO_2. Results of this study which suggest late syenitic rocks record lower P_{H_2O} during crystallization and the presence of intercumulus carbonate in OS and JLP cumulates supports this model. Further refinement of fluid conditions during melting will be an important constraint on the tectonic processes controlling magmatism in the late Archean.

Conclusions

The late Archean amphibole-bearing plutonic suites examined in this study range in composition from tonalite to syenite but share common field, mineralogical, and compositional attributes. These rocks and associated mafic units crystallized from juvenile magma introduced into the crust in substantial volume during the Late Archean. These plutons are the products of a range of parental magma compositions which subsequently fractionated amhibole and subordinate plagioclase. In the southern Superior Province the plutonic rocks record a secular change from ~2.70 Ga tonalitic intrusions to ~2.68 Ga syenitic rocks, which may be a result of progressively less hydrous mantle sources.

Elemental geochemical characteristics of the plutons examined in this study are consistent with Shirey and Hanson's (1984) isotopic and elemental constraints suggesting that monzodioritic late-Archean magmas are derived from time-averaged depleted mantle sources that were enriched in LILE shortly before melting. Refinement of potential sources of mantle enrichment are necessary before the processes of magma genesis can be fully constrained. An analogy with modern subduction regimes is tempting, however, in view of petrological comparisons with plutonic rocks of modern terrains and structural studies of Archean rocks that suggest subprovinces are accreted terrains (Percival and Williams 1989).

Acknowledgements. E. Ambrose is thanked for computer assistance. S. Trepannier is thanked for processing mineral separates, point counting and technical assistance. Critical reviews by P.C. Thurston, G.P. Beakhouse, C.T. Barrie and two anonymous referees resulted in improvements to the manuscript. K. Gil drafted the figures. Work by RHS on the Jackfish Lake Pluton formed part of an M. Sc thesis at the University of Toronto supervised by J.J. Fawcett with financial support from EMR (Research Agreements 203-4-78 and 222-4-79), OGS, and an NRC scholarship. R.H.S., A.R.S. and W.D. publish with permission of the Director. Ontario Geological Survey.

References

Arth JG (1976) Behavior of trace elements during magmatic processes: A summary of theoretical models and their applications. J Res US Geol Surv 4:41–47

Arth JG, Hanson GN (1972) Quartz diorites derived by partial melting of eclogite or amphibolite at mantle depths. Contrib Mineral Petrol 37:161–174

Arth JG, Hanson GN (1975) Geochemistry and origin of early Precambrian crust of northeastern Minnesota. Geochim Cosmochim Acta 30:325–362

Arth JG, Barker F, Peterman ZE, Friedman I (1978) Geochemistry of the gabbro – diorite – tonalite – trondhjemite suite of southwest Finland and its implications for the origin of tonalitic and trondhjemitic magmas. J Petrol 19:289–316

Barker F, Arth JG (1976) Generation of trondhjemitic – tonalitic liquids and Archean bimodal trondhjemite – basalt suites. Geology 4:596–600

Barrie CT, Shirey SB (1989) Geochemistry and Nd – Sr isotope systematics of the Kamiskotia area, western Abitibi Subprovince, Canada: implications for mantle processes during the formation of the southern superior craton (abstract). Lunar Planet Inst Workshop on the Archean mantle, pp 11–13

Basu AR, Goodwin AM, Tatsumoto M (1984) Sm – Nd study of Archean alkalic rocks from the Superior Province of the Canadian Shield. Earth Planet Sci Lett 70:40–46

Bender JF, Hanson GN, Bence AE (1984) Cortlandt Complex: differentiation and contamination in plutons of alkali basalt affinity. Am J Sci 284:1–57

Bickle MJ (1978) Heat loss from the earth: a constraint on Archean tectonics from the relation between geothermal gradients and rate of plate production. Earth Planet Sci Lett 40:301–315

Blackburn CE (1976) Geology of the Off Lake-Burditt Lake Area, District of Rainy River, Ontario Division of Mines, Geol Rep 140:62

Cameron EM, Hattori K (1987) Archean gold mineralization and oxidized hydrothermal fluids. Econ Geol 82:1177–1191

Corfu F, Krogh TE, Kwok YY, Marmont S, Jensen LS (1989) U–Pb zircon geochronology in the south-western Abitibi greenstone belt, Superior Province. Can J Earth Sci 26:1747–1763

Doherty W (1989) An internal standardization procedure for the determination of yttrium and the rare earth elements in geological materials by inductively coupled plasma-mass spectrometry. Spectrochim Acta 48B:263–280

Edgar AD (1983) Relation of ultrapotassic magmatism in the western USA to the Yellowstone plume. Neues Jahrb Mineral Abh 147:35–46

Edwards GR (1983a) Geology of the Bethune Lake Area, Districts of Kenora and Rainy River. Ontario Geol Surv, Geol Rep 201:59

Edwards GR (1983b) Geology of the Straw Lake Area, Districts of Kenora and Rainy River. Ontario Geol Surv Geol Rep 222:67

Ellam RM, Hawkesworth CJ (1988) Elemental and isotopic variations in subduction related basalts: evidence for a three component model. Contrib Mineral Petrol 98:72–80

Fowler MB (1988) Ach'uaine hybrid appinite pipes: evidence for mantle-derived shoshonitic parent magmas in Caledonian granite genesis. Geology 16:1026–1030

Frey FA, Chappell BW, Roy SD (1978) Fractionation of rare-earth elements in the Tuolumne Intrusive Series, Sierra Nevada Batholith, California, Geology 6:239–242

Fyon JA, Troop DG, Marmont S, Macdonald AJ (1989) Introduction of gold into Archean crust, Superior Province, Ontario: coupling between mantle initiated magmatism and lower crustal thermal maturation. Econ Geol Monogr 6:479–490

Furman T, Spera FJ (1985) Co-mingling of acid and basic magmas with implications for the origin of mafic I-type xenoliths: field and petrochemical relations of an unusual dike complex at Eagle Lake, Sequoia National Park, California, USA. J Volcanol Geotherm Res 24:151–178

Gariepy C, Allegre CJ (1985) The lead isotope geochemistry and geochronology of late kinematic intrusives from the Abitibi greenstone belt, and the implications for late Archean crustal evolution. Geochim Cosmochim Acta 49:2371–2383

Gerlach DC, Grove TL (1982) Petrology of Medicine Lake Highland volcanics: characterization of endmembers of magma mixing. Contrib Mineral Petrol 80:147–159

Green TH (1982) Anatexis of mafic crust and high pressure crystallization of andesite. In: Thorpe RS (ed) Andesites: Orogenic andesites and related rocks. J Wiley and Sons Ltd, pp 465–488

Gupta VK, Sutcliffe RH (1990) Mafic-ultramafic intrusives and their gravity field, Lac des Iles area, northern Ontario. Geol Soc Am Bull, in press

Haskin LA, Haskin MA, Frey FA (1968) Relative and terrestial abundances of the rare earths. In: Ahrens LH (ed) Origin and Distribution of the Elements. Pergamon, Oxford, pp 889–912

Hammarstrom JM, Zen E-An (1986) Aluminum in hornblende: an empirical igneous geobarometer. Am Mineral 71:1297–1313

Hyndman DW, Foster DA (1988) The role of tonalites and mafic dikes in the generation of the Idaho batholith. J Geol 96:31–46

Jaques AL, Green DH (1980) Anhydrous melting of peridotite at 0–15 kb pressure and the genesis of tholeiitic basalts. Contrib Mineral Petrol 73:287–310

Kushiro I (1972) Effect of water on the composition of magmas formed at high pressures. J Petrol 13:311–334

Leake BE (1978) Nomenclature of amphiboles. Can Mineral 16:501–520

Longstaffe FJ, McNutt RH, Crocket JH (1982) Rare-earth element modelling of Archean meta-igneous and igneous rocks, Lake Despair area, northwestern Ontario. Precambrian Res 17:275–296

Longstaffe FJ, McNutt RH, Schwarcz HP (1980) Geochemistry of the Archean Lake Despair area, Wabigoon Subprovince, northwestern Ontario. Can J Earth Sci 17:1046–1063

Lovell HL (1972) Geology of Eby and Otto area, District of Timiskaming. Ontario Department of Mines and Northern Affairs, Geol Rep 99:34

Martin H (1986) Effect of steeper Archean geothermal gradient on geochemistry of subduction zone magmas. Geology 14:753–756

McMillan NJ, Dungan MA (1986) Magma mixing as a petrogenetic process in the development of the Taos Plateau volcanic field, New Mexico. J Geophys Res 91:6029–6045

Morse SA (1970) Alkali feldspars with water at 5 kb pressure. J Petrol 11:221–251

Mortensen JK (1987) Preliminary U–Pb zircon ages for volcanic and plutonic rocks of the Noranda-Lac Abitibi area, Abitibi Subprovince, Quebec. In: Current Research, Part A. Geol Surv Can Pap 87-1A, pp 581–590

Mysen BO, Boettcher AL (1975) Melting of hydrous mantle: II. Geochemistry of crystals and liquids formed by anatexis of mantle peridotite at high pressures and temperatures as a function of controlled activities of water, hydrogen and carbon dioxide. J Petrol 16:549–593

Mysen BO, Kushiro I (1977) Compositional variations in co-existing phases with degree of melting of peridotite in the upper mantle. Am Mineral 62:843–865

Ontario Geol Surv (1990) Geological Map of Ontario. Scale 1:1,000,000. PC Thurston (ed), in press

Peacock MA (1931) Classification of igneous rock series. J Geol 39:54–67

Percival JA, Williams HR (1989) Late Archean Quetico accretionary complex, Superior Province, Canada. Geology 17:23–25

Presnall DC, Dixon JR, O'Donnell TH, Dixon SA (1979) Generation of mid-ocean ridge tholeiites. J Petrol 20:3–35

Reid JB, Evans OC, Fates DG (1983) Magma mixing in granitic rocks of the central Sierra Nevada, California. Earth Planet Sci Lett 73:306–316

Rock NMS, Groves DI (1988) Can lamprophyres resolve the genetic controversy over mesothermal gold deposits? Geology 16:538–541

Shirey SB, Hanson GN (1984) Mantle-derived Archean monzodiorites and trachyandesites. Nature 310:222–224

Shirey SB, Hanson GN (1986) Mantle heterogeneity and crustal recycling in Archean granite-greenstone belts: evidence from Nd isotopes and trace elements in the Rain Lake area, Superior Province, Ontario, Canada. Geochim Cosmochim Acta 50:2631–2651

Silver LT, Chappell BW (1988) The Peninsular Ranges Batholith: an insight into the evolution of Cordilleran batholits of southwestern North America. Trans R Soc Edinburg, Earth Sci 79:105–121

Smith AR, Sutcliffe RH (1988) Plutonic rocks of the Abitibi Subprovince. In: Ontario Geol Surv, Summary of Field Work and Other Activities (1988) Misc Pap 141:188–196

Stern RA, Hansen GN, Shirey SB (1989) Petrogenesis of mantle-derived, LILE-enriched Archean monzodiorites and trachyandesites (sanukitoids) in the southwestern Superior Province. Can J Earth Sci 26:1688–1712

Stormer JC, Nicholls J (1978) XLFRAC: A program for interactive testing of magmatic differentiation models. Computers and Geosci 4:143–159

Streckeisen A (1976) To each plutonic rock its proper name. Earth-Sci Rev 12:1–33

Sutcliffe RH (1989) Magma mixing in late Archean tonalitic and mafic rocks of the Lac des Iles area, western Superior Province. Precambrian Res 44:81–101

Sutcliffe RH, Sweeny JM, Edgar AD (1989) The Lac des Iles Complex, Ontario: petrology and PGE mineralization in an Archean mafic intrusion. Can J Earth Sci 26:1408–1427

Sutcliffe RH, Fawcett JJ (1980) Petrological studies on the Rainy Lake granitoid complex: A preliminary evaluation. In: Geol Surv Can, Current Res, Pap 80-1A:335–338

Tuttle OF, Bowen NL (1958) Origin of granite in light of experimental studies in the system $NaAlSi_3O_8-KAlSi_3O_8-SiO_2-H_2O$. Geol Soc Am Mem 74:153

Whalen JB (1985) Geochemistry of an island arc plutonic suite: the Uasilau Yau-Yau Intrusive Complex, New Britain, Papua New Guinea. J Petrol 26:603–623

Wones DR (1981) Mafic silicates as indicators of intensive variables. Min Geol (Jap) 31:191–212

Wones DR, Dodge FCW (1977) The stability of phlogopite in the presence of quartz and diopside. In: Fraser DG (ed) Thermodynamics in Geology. Reidel Publishing Company, Dordrecht, Holland, pp 229–247

Wyllie PJ (1977) Crustal anatexis: an experimental review. Tectonophysics 43:41–71

Wyman DA, Kerrich R (1989) Archean lamprophyre dikes of the Superior Province, Canada: distribution, petrology and geochmical characteristics. J Geophys Res 94 n B4:4667–4696

Wyman DA, Kerrich R (1988) Alkaline magmatism, major structures and gold deposits: implications for greenstone belt and gold metallogeny. Econ Geol 83:451–456

Zen E-An (1986) Aluminum enrichment in silicate melts by fractional crystallization: some mineralogic and petrographic constraints. J of Petrol 27:1095–1117

Editorial responsibility: T. Grove